(4)

NUSC Technical Report 8389
29 September 1988

Turbulent Boundary Layer on a Cylinder in Axial Flow

Richard M. Lueptow
Submarine Sonar Department

Naval Underwater Systems Center
Newport, Rhode Island / New London, Connecticut

Preface

This report was prepared by Richard M. Lueptow (Code 2141) during tenure as a fellow in the NAVY/ASEE Summer Faculty Research Program at the Naval Underwater Systems Center. The technical reviewer for this work was Dr. David Hurdis (Code 2141).

The author gratefully acknowledges the support of the NAVY/ASEE Summer Faculty Research Program. Also, the author wishes to thank Dr. Henry Bakewell and Dr. David Hurdis for the opportunity to pursue this work.

Reviewed and Approved: 29 September 1988

F. V. Kingsbury

F. J. Kingsbury
Head: Submarine Sonar Department

UNCLASSIFIED
SECURITY CLASSIFICATION OF THIS PAGE

REPORT DOCUMENTATION PAGE

1a. REPORT SECURITY CLASSIFICATION: UNCLASSIFIED	1b. RESTRICTIVE MARKINGS
2a. SECURITY CLASSIFICATION AUTHORITY	3. DISTRIBUTION/AVAILABILITY OF REPORT: Approved for public release; distribution is unlimited.
2b. DECLASSIFICATION/DOWNGRADING SCHEDULE	
4. PERFORMING ORGANIZATION REPORT NUMBER(S): NUSC TR 8389	5. MONITORING ORGANIZATION REPORT NUMBER(S)
6a. NAME OF PERFORMING ORGANIZATION: Naval Underwater Systems Center; 6b. OFFICE SYMBOL (If applicable): 2141	7a. NAME OF MONITORING ORGANIZATION
6c. ADDRESS (City, State, and ZIP Code): New London Laboratory, New London, CT 06320	7b. ADDRESS (City, State, and ZIP Code)
8a. NAME OF FUNDING/SPONSORING ORGANIZATION: Naval Underwater Systems Center; 8b. OFFICE SYMBOL (If applicable): 214	9. PROCUREMENT INSTRUMENT IDENTIFICATION NUMBER
8c. ADDRESS (City, State, and ZIP Code): New London Laboratory, New London, CT 06320	10. SOURCE OF FUNDING NUMBERS: PROGRAM ELEMENT NO.; PROJECT NO. B60010; TASK NO.; WORK UNIT ACCESSION NO.

11. TITLE (Include Security Classification)
TURBULENT BOUNDARY LAYER ON A CYLINDER IN AXIAL FLOW

12. PERSONAL AUTHOR(S)
Richard M. Lueptow

13a. TYPE OF REPORT	13b. TIME COVERED FROM TO	14. DATE OF REPORT (Year, Month, Day)	15. PAGE COUNT
		1988 September 29	62

16. SUPPLEMENTARY NOTATION
→This report reviews research←

17 COSATI CODES			18. SUBJECT TERMS (Continue on reverse if necessary and identify by block number)
FIELD	GROUP	SUB-GROUP	Turbulent Boundary Layer

19. ABSTRACT (Continue on reverse if necessary and identify by block number)

Research on the turbulent boundary layer that develops on a cylinder in axial flow is reviewed in this report. Experimental results indicate that the transverse curvature results in a higher coefficient of friction and a fuller velocity profile than for a planar boundary layer. However, appropriate scaling laws and nondimensional scaling parameters are still elusive. The few turbulence measurements such as Reynolds stress and intermittency that are available for a cylindrical boundary layer suggest that the distribution of turbulent quantities in the boundary layer is somewhat different from a planar boundary layer, particularly as the boundary layer becomes thick compared to the radius of the cylinder. This is most likely a result of the tendency for a cylindrical boundary layer to become wake-like as the cylinder becomes very small. Measurements of turbulence intensity and detection of turbulence-generating events in a cylindrical boundary layer suggest that the mechanism for the production of turbulence

20. DISTRIBUTION/AVAILABILITY OF ABSTRACT: ☒ UNCLASSIFIED/UNLIMITED ☐ SAME AS RPT. ☐ DTIC USERS	21. ABSTRACT SECURITY CLASSIFICATION: UNCLASSIFIED
22a. NAME OF RESPONSIBLE INDIVIDUAL: David A. Hurdis	22b. TELEPHONE (Include Area Code): (203)440-6497; 22c. OFFICE SYMBOL: 2141

DD FORM 1473, 84 MAR — 83 APR edition may be used until exhausted. All other editions are obsolete.

SECURITY CLASSIFICATION OF THIS PAGE
UNCLASSIFIED

19. (Continued)

near the wall is similar to that for other wall-bounded flows. However, there is experimental evidence that the outer flow interacts with the near-wall flow to modify the generation of turbulence. Suggestions for further work include more comprehensive and sophisticated measurements of turbulent quantities in cylindrical boundary layers as well as computational modeling. (edc)

TABLE OF CONTENTS

LIST OF ILLUSTRATIONS

LIST OF TABLES

THE TURBULENT BOUNDARY LAYER ON A CYLINDER IN AXIAL FLOW

1. INTRODUCTION

The effect of transverse curvature on the turbulent boundary layer that develops as a fluid flows parallel to a cylindrical surface has applications in several different fields. Early interest in the effect of transverse curvature resulted from efforts to develop frictional resistance similarity laws to allow scaling from models to full-scale for ship hulls.[1] Other early interest was in the boundary layer that develops on cylindrical missiles[2] or during the towing of submerged cables or cylindrical bodies.[3] Finally, interest in the drag of glass or polymer fibers moving through air during fabrication motivated early research.[4]

Like the planar boundary layer, the cylindrical boundary layer is two-dimensional in the streamwise and wall-normal directions, while it is periodic in the spanwise direction. However, most boundary layer research has been concentrated on the planar boundary layer. In spite of the apparent simplicity of an axisymmetric boundary layer, the volume of research and, hence, the level of understanding regarding the physics of this boundary layer have lagged behind that of planar boundary layers.

Upon further investigation, an axisymmetric boundary layer is not as simple as its two-dimensional character implies because of the existence of an additional length scale, the radius of transverse curvature, a. This additional length scale suggests several nondimensional parameters, i.e., $a_+ = a\,U_\tau/\nu$, δ/a, $R_a = a\,U_\infty/\nu$, and $\xi = \sqrt{(\nu\,x/U_\infty a^2)}$. The first scaling parameter, a_+, is a wall scaling based on the friction velocity, U_τ, and the kinematic viscosity, ν.* The second scaling parameter is a transverse curvature ratio relating the boundary layer thickness, δ, with the radius of transverse curvature of the surface. The third scaling parameter mixes the outer free stream velocity, U_∞, with the transverse curvature resulting in a Reynolds number based on transverse curvature, R_a. The last scaling parameter incorporating the streamwise coordinate, x, was proposed in conjunction† with the laminar axisymmetric boundary layer.[5] Note that all of these scaling parameters except R_a are "local" with respect to the flow. In other words, they depend upon U_τ, δ, or x which, in turn, depend upon the streamwise position in the boundary layer. Only R_a is independent of the streamwise location in the boundary layer.

---

* All variables subscripted with + have been nondimensionalized using ν and $U_\tau = \sqrt{(\tau_w/\rho)}$, where τ_w is the wall shear stress and ρ is the fluid density.

† Seban and Bond[5] indicate that the parameter ξ was originally proposed by Young,[6] although this reference was not available to the author for confirmation.

Consider the extreme cases of transverse curvature. First, as the radius of transverse curvature, a, approaches infinity (a_+ and R_a very large; δ/a and ξ very small), the boundary layer should be similar to a planar boundary layer. A similar result occurs when the boundary layer thickness is very small compared with the radius of transverse curvature resulting in small δ/a. On the other hand, if the radius of transverse curvature, a, is very small (a_+ and R_a small; δ/a and ξ large) the boundary layer can be much thicker than the diameter of the cylinder. For instance, Richmond[7] measured the cylindrical boundary layer to be nearly an inch (2.5 cm) thick on a wire with a radius of 0.012 inches (0.03 cm). Denli and Landweber[8] note that as δ/a increases, the outer flow in a cylindrical boundary layer becomes increasingly independent of the wall suggesting a flow that would be similar to a cylindrical wake with a modified inner boundary condition.

The range of experimental data that is available for the mean velocity profile is shown in figure 1 in of terms various scaling parameters. In addition, the Reynolds number based on momentum thickness, R_θ, is included, since this parameter is also defined for planar boundary layers. The range of measurements for a_+ and R_a span three orders of magnitude, but the same measurements only represent a range of one or two orders of magnitude for δ/a and ξ. Luxton et al.[9] show a logarithmic correspondence between a_+ and R_a for available experimental data. * Their figure also shows that as a_+ and R_a increase, δ/a decreases for the available experimental data. The direct relation between a_+ and R_a is primarily a result changing the radius of transverse curvature or the free stream velocity to obtain a variation in scaling parameters. Using this approach, a_+, δ/a, and R_a are not independently varied. Very little data are available based on parameter variation accomplished by measuring the boundary layer characteristics at different axial locations given the same transverse curvature in order to vary a_+ and δ/a while keeping R_a constant. Because data obtained in this way are scarce, proper scaling parameters have been difficult to identify.

At this point it is necessary to discuss a nuance in the terminology that is often overlooked. The terms "axisymmetric boundary layer" and "cylindrical boundary layer" have been used interchangeably to describe a boundary layer that develops as a fluid flows parallel to the axis of a cylinder. As will become evident shortly, obtaining axial symmetry experimentally is very difficult. The problem becomes increasingly acute as the boundary layer becomes thick with respect to the radius of the cylinder. Because the boundary layer that develops on a cylinder in axial flow is not necessarily axisymmetric, the term "cylindrical" instead of "axisymmetric" will be used to describe this boundary layer.

---

*The labels on the axes of figure1 of Luxton et al.[9] are inadvertently reversed and should be interchanged.

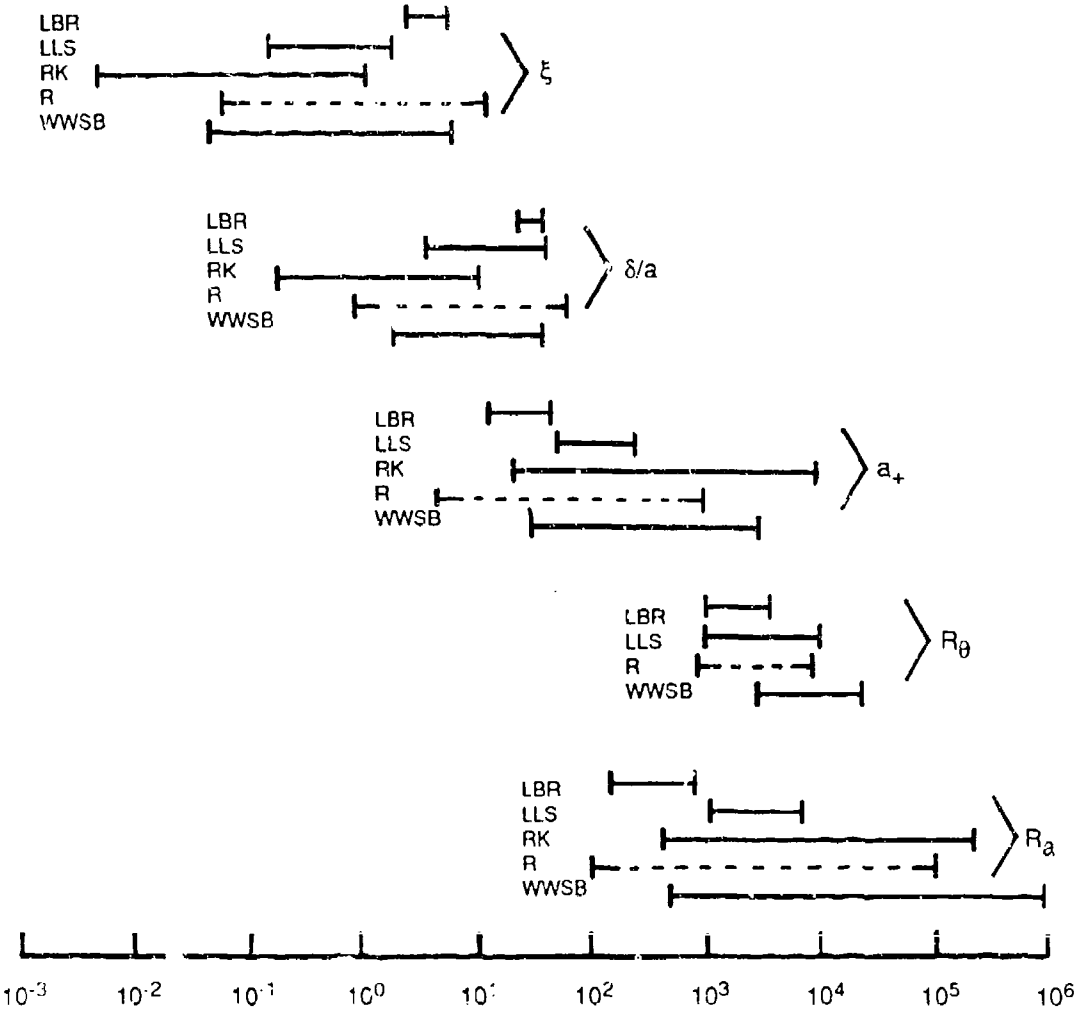

Fig. 1 Range of Values of Nondimensional Parameters for Which Mean Velocity Data for a Cylindrical Boundary Layer Are Availaole

(LBR = Luxton et al.,[9] LLS = Lueptow et al.,[10] RK = Rao and Keshavan,[11] R=Richmond,[7] WWSB = Willmarth et al.[12])

2. MEAN VELOCITY PROFILE

The differences between the mean velocity profiles for a cylindrical boundary layer and a planar boundary layer are substantial, especially as the radius of transverse curvature becomes small. This is evident in the velocity defect data of Willmarth et al.[12] reproduced in figure 2. For the larger cylinders (corresponding to a small δ/a) the velocity defect profile is nearly identical to the profile for a flat plate. As the cylinder diameter becomes smaller (corresponding to larger δ/a), the velocity defect profiles become fuller. Richmond[7] and Willmarth and Yang[14] suggest that this characteristic is similar to that for a laminar axisymmetric boundary layer. Glauert and Lighthill[15] note that in a laminar cylindrical boundary layer the shear force per unit length on a cylinder equals the circumference times the shear stress, and that this force is the same on all cylindrical fluid surfaces near the wall (see equation 2-1). Consequently, the shear stress must vary with 1/r, where r is the radial coordinate. Since the shear stress is proportional to $\partial U/\partial r$ (where U is the mean velocity in the streamwise direction), then $\partial U/\partial r$ must also vary with 1/r. As the cylinder radius becomes smaller, 1/r can become larger so the velocity gradient increases. Thus, a fuller velocity profile results as the radius of the cylinder decreases.

The differences between a planar boundary layer and a cylindrical boundary layer are also evident when the mean velocity is plotted as a function of the distance from the wall in the usual wall coordinates, U_+ and y_+ as shown in figure 3. As δ/a increases, the cylindrical mean velocity profiles drop below the planar profile. For small δ/a, the log region of the mean velocity profile nearly matches the log region for a planar boundary layer.

2.1 MEASUREMENTS OF THE WALL SHEAR STRESS

Although it may seem premature to describe measurements of the wall shear stress at this point, it is necessary to do so because the friction velocity appears in the scaling of the mean velocity profiles when presenting the mean velocity profile in wall coordinates. However, a major weakness in the presentation, analysis, and use of nearly all of the velocity data for cylindrical boundary layers is the difficulty in measuring the wall shear stress, τ_w. Although techniques have been developed for use in measuring the wall shear stress in a planar boundary layer, these methods are not directly applicable to a cylindrical boundary layer because of the effect of transverse curvature.

Richmond[7] made an attempt to measure the skin friction directly on a 0.25 inch (0.64 cm) diameter cylinder using a floating element with an inductance coil position transducer. The measured coefficient of friction for hypersonic flow is higher than that for a planar boundary layer at the same

momentum thickness Reynolds number. The skin friction was not measured for incompressible flow.

In several studies the coefficient of drag of a cylinder in axial flow was measured directly. These experimental studies fall into three categories. The first category is that of towing experiments where a cylindrical body of finite length is towed through a fluid. Unfortunately, in several of these tests it is unclear whether the flow was laminar or turbulent. Kempf[17] and Hughes[18] towed neutrally buoyant cylinders up to 84 ft (26 m) long in a water tow tank and measured the total drag. These results showed that the coefficient of friction decreases as a function of both the length-to-diameter ratio and the length Reynolds number, $R_L=U_\infty L/\nu$, where L is the length of the cylinder. Zajac[19] carried out similar tests on smooth- and rough-surfaced cables that were not neutrally buoyant, although the length-to-diameter ratio was not varied (see reference 3 for these results in terms of the diameter Reynolds number). Towing tests of optical fibers and monofilaments were carried out by Kennedy et al.[20] By using fibers as small as 0.2 mm diameter and 60 to 70 m long, the drag coefficient for very large length-to-diameter ratios and a wide range of diameter Reynolds numbers were measured. Their results indicate that the average coefficient of friction decreases as the diameter Reynolds number or the length-to-diameter ratio increases. However, because of the very small diameter of the fibers that were used, the wake of the tow body and support strut may have influenced the drag over the portion of the fiber immediately behind them.

In the second category of direct drag measurement, cylinders were suspended in a wind tunnel and the coefficient of drag was measured directly. Again the degree to which the flow field was turbulent in these tests is difficult to ascertain. Andrews and Cansfield[21] measured the drag force per unit length in this way although experimental details are sketchy. Gould and Smith[22] measured the coefficient of drag on monofilaments ranging from 8.5 μm to 150 μm in diameter and 91 cm long. At higher diameter Reynolds numbers the length-to-diameter ratio had little effect on the drag coefficient. However, at lower diameter Reynolds numbers, the drag coefficient appears to have some dependence upon the length-to-diameter ratio. Ni and Hansen[23] estimated the drag on a flexible cylinder in a water tunnel by measuring the elongation of the cylinder and correlating that elongation to an equivalent axial load.

The third category of direct drag measurement has been in connection with the tension of polymer or glass fibers during production. Typically, the tension of a continuously extruding fiber is measured using a tensiometer. The aerodynamic drag on a fiber is found by subtracting the effects of gravity, rheological drag, surface tension, and inertia from the total tension force.[24] Because the fibers are very small, the transverse curvature is certain to play a large role. In some cases, δ/a can be

estimated to be as large as of the order of 200.[25] The results of several experiments of this type show that the drag coefficient decreases with increasing radius Reynolds number, Re_a.[26-29] Unfortunately, these drag coefficient measurements are subject to question for two reasons. First, it is often unclear whether the flow is laminar, transitional, or turbulent. Second, the effect of the transverse vibration of the filament is unknown.

An indirect method of evaluating the wall shear stress in cylindrical boundary layers has been through the use of a Preston tube, a circular impact pressure tube in contact with the wall. Willmarth et al.[12] found that as long as the cylindrical boundary layer profile coincides with the planar profile the wall shear stress can be measured using a Preston tube, although the Preston tube diameter must be less than 0.3 times the cylinder diameter. Using this method, they found that the coefficient of friction generally decreases with increasing Re_a, Re_θ, and a_+, but is consistently larger than the coefficient of friction for a flat plate boundary layer. Similar results were reported by Willmarth and Yang[14] and Yu.[30] For very small cylinders Willmarth et al. were not confident of results obtained using a Preston tube because of differences between the planar velocity profile and the cylindrical velocity profile.

The inherent weakness in the use of a Preston tube is that the calibration data for a flat plate must be assumed valid for a cylindrical boundary layer. Since a Preston tube extends well into the log region of the boundary layer, and the log region of a cylindrical boundary layer is significantly different from that of a planar boundary layer for large δ/a, the validity of the flat plate calibration is questionable for small diameter cylinders. To avoid this problem, Lueptow and Haritonidis[31] used a modified impact pressure probe so small that the opening was within the sublayer. Because of the small difference in the sublayer velocity profiles for the planar case and the cylindrical case, they assumed that the planar calibration could be used for the cylindrical boundary layer measurements. Using this method, they found the wall shear stress to be greater than the planar boundary layer values and to decrease with increasing Re_x.

Several indirect measures of the wall shear stress have been used. The most common method is the use of a Clauser plot[13] to match the slope of the log region of the mean velocity profile to that for the planar case (see for example reference 32). This method will certainly provide inappropriate results when the radius transverse curvature is small, because the planar and cylindrical log region profiles are known to be different.

Willmarth et al [12] and Lueptow et al.[10] used a method in which the measured mean velocity profile data in the sublayer and buffer zone were fitted to the planar sublayer profile through the

adjustment of the friction velocity, thus specifying the wall shear stress. The assumption here was that very close to the wall the differences between a planar profile and a cylindrical profile are negligible. Willmarth et al. verified this assumption for $\delta/a < 10$ by comparing the wall shear stress obtained using this method with the wall shear stress measured using a Preston tube. However, Lueptow and Haritonidis[31] found that matching the mean velocity profile to the sublayer profile resulted in wall shear stresses that were higher than those measured with their sublayer impact pressure probe.

Lueptow et al.,[10] noting the relationship between the Reynolds stress and the wall shear stress in a cylindrical boundary layer (see equations 2-1 and 2-2), used the slope of the Reynolds stress profile when plotted as a function of a/r to estimate the wall shear stress. Although this method shows trends consistent with other methods, the scatter in the data is too large to make this a useful technique for finding the wall shear stress.

Finally, it should be noted that the wall shear stress can be found from the streamwise gradient of the momentum integral expression for an axisymmetric boundary layer after substitution of experimental velocity profiles into the integral (see equation 2-7). Afzal and Singh[32] used this method and obtained results similar to those obtained using Clauser plots for small δ/a. In practice, this procedure is erroneous unless perfect axisymmetry is maintained as pointed out by Lueptow et al.[10] Errors related to the differentiation of experimentally derived quantities is also a problem with this method.

2.2 COMMENTS ON EXPERIMENTAL METHODS FOR VELOCITY MEASUREMENTS IN CYLINDRICAL BOUNDARY LAYERS

Most experimental setups used to make velocity measurements of cylindrical boundary layers involve the suspension of a cylindrical model along the centerline of a wind tunnel and the measurement of the velocities in the boundary layer using hot wire anemometry. This approach brings about a host of experimental problems. Most crucial perhaps, is the problem of maintaining axisymmetry of the boundary layer. In spite of holding the cylinder in tension[9] or supporting it with guy wires,[30] asymmetry of the boundary layer often results from the sag of the cylinder in a horizontal wind tunnel. The sag problem has been successfully overcome by the use of a vertical wind tunnel by Willmarth et al.[12] Even so, they experienced difficulty in finding cylinders that were straight. Apart from the sag problem is the difficulty in keeping the cylinder parallel to the air flow in the wind tunnel. Willmarth, Sharma and Inglis[33] and Lueptow et al.[10] found that an angle as small as 0.05° between the axis of the cylinder and the flow

direction can alter the boundary layer thickness substantially. Rao and Keshavan[11] investigated the growth of the momentum thickness with streamwise location for a yaw angle of 1°.

The leading edge condition is also troublesome for the experimentalist. Often a cylinder is mounted in a wind tunnel so that the cylinder extends upstream into the contraction section,[9] the settling chamber,[12] or outside of the wind tunnel[10] to create an intentionally ambiguous leading edge condition. Of course this leads to problems in defining any streamwise parameters (for example see reference 31). Sometimes it is necessary to trip the boundary layer in order to obtain turbulent flow within the test section. Lueptow et al.[10] simply used an O-ring around the cylinder at the upstream end of the test section for this purpose. A significant number of experiments have been performed with a cylinder moving through a quiescent fluid (for example reference 25). Again this experimental setup results in ambiguity in the definition of streamwise parameters and the leading edge conditions. In cases where the leading edge of the cylinder is within the test section, hemispherical[30] and ogive-shaped[11] leading edge geometries have been used.

Velocity measurements in boundary layers on very small cylinders are difficult because the length scale of the hot-wire probe or pitot tube is often of the same order as the radius of curvature. For instance, in widely referenced experiments, Richmond[7] used a 0.015 inch (0.38 mm) long hot-wire to make mean velocity measurements on a cylinder with a radius of only 0.012 inch (0.30 mm). Near the wall, the measured velocity was probably in error since the hot-wire averages the velocity over the length of the wire, and the ends of the hot-wire were exposed to higher mean velocities than the center of the wire. In addition, the midpoint of the hot-wire must be centered over the cylinder, so that it will not be exposed to different velocities at each end of the wire.

2.3 MEAN VELOCITY PROFILE IN THE VISCOUS SUBLAYER

In the sublayer region, the analysis of the mean velocity profile begins with the streamwise Navier-Stokes equation in cylindrical coordinates. Assuming there is no pressure gradient and noting that the streamwise gradients and the wall-normal velocity are small in the sublayer, the equation reduces to

$$a\tau_w = r\tau \tag{2-1}$$

The total shear stress, τ, is given by

$$\tau/\rho = \nu\ (\partial U/\partial r) - \overline{uv}\,, \qquad (2\text{-}2)$$

where ρ is the fluid density, u and v are the fluctuating velocities in the streamwise and wall-normal directions, respectively, and the overbar denotes time averaging. The second term on the right-hand side of (2-2) is the Reynolds stress which arises from the turbulent velocity fluctuations. Equation (2-1), sometimes called the constant shear moment, is analogous to the constant shear layer very near the wall in a planar boundary layer.

Reid and Wilson[3] and Rao[34] reasoned that the fluctuating velocities are small in the viscous sublayer so the Reynolds stress is negligible allowing the integration of (2-1) after substituting in (2-2). This leads to

$$U_+ = a_+ \ln(r/a). \qquad (2\text{-}3)$$

Equation (2-3) is widely accepted as the appropriate description of the mean velocity profile in the sublayer of a cylindrical boundary layer. Noting that $\ln(r/a) = \ln[1+(y/a)] \approx y/a$ for small y/a, (2-3) reduces to the planar sublayer expression, $U_+ = y_+$, when the radius of curvature, a, is large.

Experimental verification of equation (2-3) is difficult since, like the planar sublayer expression, this expression is valid only out to a distance from the wall of $y_+ < O(10)$. Velocity measurement is very difficult this close to a surface because of heat transfer to the wall, probe resolution, and accurate calibration at very low velocities. Nevertheless, Willmarth et al.[12] showed that very near the wall ($y_+ \leq 5$) the data appear to fall on the curve defined by equation (2-3) as shown in figure 3. In that same figure, it is evident that equation (2-3) is not significantly different from the planar sublayer profile, even for the smallest a_+ that Willmarth et al. measured.

2.4 MEAN VELOCITY PROFILE IN THE INNER REGION

Away from the wall, outside the viscous sublayer, is the inner region of flow where the influence of the wall is important, yet viscous shear stresses do not dominate. The equivalent region in a planar boundary layer is often called the log region. Many attempts have been made at the measurement of the mean velocity profile in the inner region as indicated in table 1. Several of these studies were flawed by insufficient probe resolution as noted in the table. Of course, the problem of probe resolution is exaggerated for the very situation where the effects of transverse curvature are

greatest – for small cylinders where the length scale of the probe can easily approach the scale of the transverse curvature. As mentioned earlier, the determination of the wall shear stress is also experimentally difficult. The methods that were used are noted in the table.

Three methods of scaling the wall-normal coordinate have been commonly used for the mean velocity profile data. The first method is to use the planar wall-normal coordinate, y_+. When this scaling is used for small δ/a the results are very similar to those for a flat plate boundary layer,[32,41] although there is some indication that the coefficients of the planar log law must be adjusted to fit the data.[30,37] As the curvature ratio, δ/a, increases, the logarithmic relationship for the mean velocity profile remains intact,but the slope of the logarithmic region deviates from the planar log law[9,10,12] as shown in figure 3. To quantify this effect, Lueptow et al.[10] compiled data from several sources and assumed a log law of the same form as the planar case, i.e.,

$$U_+ = (1/m) \ln y_+ + n. \qquad (2\text{-}4)$$

They found that as $\delta/a \rightarrow 1$, m approaches its planar value of $\kappa=0.4$, the Von Karman coefficient. Likewise, n approaches its planar value of 5.0 as $\delta/a \rightarrow 1$. Both coefficients increase with increasing δ/a. In fact, m is a linear function of δ/a. This linear relationship appears to break down for $\delta/a>40$, perhaps because of experimental problems when measuring profiles on extremely small cylinders or because of relaminarization.

This result is not surprising in light of the increased coefficient of friction measured (and predicted, as seen in later sections) for cylindrical boundary layers. Recall that the coefficient of friction can be expressed in terms of the friction velocity as $C_f=2\,(U_\tau/U_\infty)^2$. If the coefficient of friction is larger in a cylindrical boundary layer than in a planar boundary layer, then the nondimensional free stream velocity, U_∞/U_τ, must be smaller. Unless the nondimensional cylindrical boundary layer thickness, δ_+, is much smaller than in the planar case, the slope of the log region of a cylindrical velocity profile must be less than that of a flat plate profile.

Table 1. Measurements of the Mean Velocity Profile in the Cylindrical Boundary Layer (Values for δ/a and x/a were estimated based on information presented in each paper. The studies listed are in order of decreasing curvature ratio, δ/a. The ratio x/a, where x is the axial position of the measurement, typically decreases as the curvature ratio increases because of experimental constraints.)

Ref.	Number of Profiles	Measurement Method	Wall Shear Stress Method	δ/a	x/a	Wall-Normal Coordinates Used(a)	Notes
25	4	hot-wire (b)	-	200	100000	dimensional	continuous cylin. outer region
7	7	hot-wire (b)	match sublayer profile	1→72	192→ 16000	Richmond	subsonic & supersonic
10	6 (c)	hot-wire	match sublayer profile	4→47	150→ 4300	planar	-
9	3	pitot (b)	Ref. 12 Fig. 8	26→42	400→ 5644	planar	very small a+
12	6 (d)	hot-wire	Preston tube; match sublayer profile	2→42	220→ 22000	planar	-
11	42	pitot (b)	momentum integral	0.3→13	6→640	Rao	-
35	8 (e)	pitot (b)	-	1→5	10→770	outer	water tunnel results
36	6	hot-wire (b)	Clauser plot	0.5→3	16→ 412	Rao	effect of free-stream turb.
37	3	pitot	momentum integral	2	80	planar	-
14	3	pitot	Preston tube	2	192→ 288	Richmond	-
32	6	pitot	Clauser plot; momentum integral	0.4→ 2	35→ 150	planar	-
38	1	pitot	?	1	175	Richmond	-
30	14	pitot	Preston tube	1	24→84	planar	-
39	4	pitot	?	0.3	9→19	Richmond	rotating cylinder

Table 1. (Cont'd) Measurements of the Mean Velocity Profile in the Cylindrical Boundary Layer

Ref.	Number of Profiles	Measurement Method	Wall Shear Stress Method	δ/a	x/a	Wall-Normal Coordinates Used	Notes
40	12	?	Clauser plot	0.3	2→9	Rao	adverse & favor. pressure grad.
41	3	hot-wire	?	0.2	8→11	planar	rotating cylinder
33	3	pitot	-	2→9	216	-	isovelocity contours for yaw

Notes:

a) Key for wall-normal coordinates:

Dimensional	y or r
Outer	y/δ
Planar	y_+
Rao	$a_+ \ln(r/a)$
Richmond	$y_+[1+(y/2a)]$

b) Poor velocity probe resolution calls the validity of the results into question, especially near the wall.

c) Lueptow et al.[10] include characterization of the mean velocity profile for over 40 profiles.

d) Willmarth et al.[12] report includes a total of 14 profiles.

e) Joseph et al.[35] include characterization of the mean velocity profile for over 60 profiles.

The mean velocity profile data described above allows the evaluation of the scaling parameters described earlier. Lueptow et al.[10] varied δ/a by making measurements at several locations along the length of a cylinder at constant R_a. Since the slope of the log region of the boundary layer profiles varied even with constant R_a, R_a seems to be an inappropriate scaling parameter for cylindrical boundary layers.

Rao[34,42] suggested that the wall-normal coordinate of the planar boundary layer log law be replaced by the corresponding wall-normal coordinate of the sublayer law for an axisymmetric boundary layer given in equation (2-3). Thus y_+ in the planar law should be replaced by $Y_+=[a_+ \ln(r/a)]$ leaving all coefficients of the planar log law intact (κ=0.4, B=5). This results in the velocity profile in the log region of a cylindrical boundary layer of

$$U_+ = (1/\kappa) \ln[a_+ \ln(r/a)] + B. \qquad (2\text{-}5)$$

Considerable controversy followed the introduction of Rao's wall-normal coordinate, Y_+. Undoubtedly, the introduction of this scale reflects the geometry of the cylindrical boundary layer. Since $Y_+ = a_+ \ln[1+(y/a)] \approx a_+(y/a) = y_+$ for large a, the flat plate logarithmic velocity profile is recovered from (2-5). Chase[43,44] supported the Rao hypothesis, since it suggests a physically meaningful mixing length that increases linearly with distance from the wall only for $y \le a$, while it increases logarithmically further out in the boundary layer. On the other hand, Bradshaw and Patel[45] point out that "there is no reason why the fully turbulent flow should respond to ... [transverse] curvature in the same way as the sublayer ..." For this reason they dismissed the success of Rao's log law (2-5) in matching experimental data as fortuitous.

Rao and Keshavan[11] measured mean velocity profiles corresponding to (2-5) for cylinder diameters ranging from 1/16 inch (0.16 cm) to 5.5 inches (14 cm). Unfortunately, poor probe resolution calls their results for small cylinders into question. This problem aside, they found that the coefficients of (2-5) to be dependent upon a_+ and R_a. Fernholz and Podtschaske[46] also suggested that the coefficients in (2-5) are not constant based on an analysis of the data obtained by Willmarth et al.[12] Instead they proposed that the coefficients are functions of a curvature ratio, θ/a, where θ is the momentum thickness. At curvature ratios of $\delta/a=O(1)$, Adomaitis[36] and Furuya et al.[40] found that the coefficients of (2-5) are the planar values, κ =0.4 and B=5.

A third scaling for the wall-normal coordinate, $\{y_+ [1+(y/2a)]\}$, was proposed by Richmond[7] based on cylindrical geometry and a hypothesis that streamlines are lines of constant mean velocity. Substituting this scaling for y_+ in the planar log law, Richmond,[7] Yasuhara,[38] Willmarth and Yang,[14] and Bissonnette and Mellor[39] found that data for the cylindrical mean velocity profile matched the planar velocity profile quite well for $\delta/a<2$. However, Richmond's data for large δ/a fell well below the planar profile in the log region. Rao[34] cast doubt on the validity of the Richmond wall-normal scaling. As a result Richmond's wall-normal scaling has been discarded in favor of the traditional planar wall-normal scaling or Rao's wall-normal scaling.

Other measurements of the mean velocity in a cylindrical boundary layer should be mentioned for completeness. Kwon and Prevorsek[25] measured the velocity profile surrounding a continuous fiber moving through quiescent air. The small diameter of the fiber resulted in a boundary layer that was at least two orders of magnitude thicker than the fiber diameter, but only measurement in the outermost portion of the boundary layer could be made because of the size of the velocity probe. Joseph et al.[35] measured the mean velocity profile for cylinders in both water and wind tunnels. In determining the exponent of a power law approximation to the mean velocity profile, they found that the exponent is dependent upon the radius of the cylinder but, curiously, is independent of the fluid viscosity. Finally, Willmarth et al.[33] measured isovelocity contours around cylinders at small angles of yaw. The boundary layer on the leeward side was nearly 10 times as thick as the boundary layer on the windward side for a yaw angle of only 1°.

In summary, it appears that the planar, Rao, and Richmond wall-normal coordinates all result in a logarithmic relationship for the mean velocity profile in the inner region of a cylindrical boundary layer, although the planar and Rao coordinates are preferred. However, no wall-normal scaling collapses data on to a single curve for all transverse curvatures. Unfortunately, much of the data suffers poor measurement techniques or small curvature ratios so that it is difficult to make conclusions on the character or scaling of the mean velocity profile for cylindrical boundary layers.

2.5 ANALYTIC MODELS OF THE VELOCITY PROFILE IN THE INNER REGION

Analytic approaches to the mean velocity profile in the inner region of a cylindrical boundary layer often depend upon the assumption of similarity with planar boundary layers, so the validity of the method depends upon the suitability of using planar boundary layer characteristics to describe a cylindrical boundary layer. Most approaches have been based upon eddy viscosity or mixing length closure schemes to account for the Reynolds stress term in (2-2). The eddy viscosity, ε, is defined so

that the representation of the turbulent shear stress is similar to the representation of the viscous shear stress. The mixing length approach relates the turbulent shear stress through a turbulent length scale, l_m. Using these closure schemes the Reynolds stress is expressed as

$$-\overline{uv} = \varepsilon \, \partial U/\partial y = l_m^2 \, |\partial U/\partial y| \, \partial U/\partial y. \qquad (2\text{-}6)$$

Of course, the eddy viscosity and mixing length are related by $\varepsilon = l_m^2 \, |\partial U/\partial y|$. Most closure schemes for cylindrical boundary layers have been presented in terms of a mixing length, so that is the format used to compare the schemes in table 2.

The earliest attempts at using a mixing length for closure were based on the direct application of the mixing length concepts used for planar boundary layers. Sparrow et al.[47] used an expression of mixing length based on Von Karman's similarity hypothesis using a local characteristic length scale based on consecutive wall-normal derivatives of the mean velocity profile.

Other early attempts used a simple planar mixing length, $l_+ = l_m U_\tau/\nu = \kappa y_+$, where κ is the Von Karman constant. In this representation the mixing length and, hence, the turbulent length scales are proportional to the distance from the wall. Ginevskii and Solodkin[48] expanded (2-1) in a Maclaurin series and then applied this mixing length to achieve a complex expression for the mean velocity profile in terms of the boundary layer thickness and δ/a. Their expression was general enough to account for either concave or convex transverse curvature. Reid and Wilson[3] also used this simple planar mixing length to derive an expression for the boundary layer velocity profile that was a function of the sublayer thickness because of a matching condition at the overlap of the sublayer and the log region. They extended their analysis to include the effect of surface roughness on the velocity profile. Bradshaw and Patel[45] carried out an analysis of the log region using a planar mixing length along with equation (2-1). Their resultant logarithmic velocity profile required an additive coefficient dependent upon a_+. Matsui[27] also used the planar mixing length to model the turbulent shear, although the constant κ was determined empirically.

The simple planar mixing length has been modified to include a factor accounting for the velocity profile in the sublayer. This allows the use of the logarithmic velocity profile in the sublayer as well as in the log region of a boundary layer velocity profile. Cebeci[49] used the Van Driest sublayer

correction[56] for the mixing length, while Patel[50] used a factor suggested by Landweber and Poreh[57] to modify the logarithmic velocity profile in the sublayer.

Table 2. Proposals for the Mixing Length for a Cylindrical Boundary Layer

Mixing Length Expression		Reference
Planar Mixing Length:		
$l_+ = \kappa\,(dU_+/dy_+) / (d^2U_+/dy_+^2)$	$\kappa = 0.4$ (planar value)	Sparrow, Eckert & Minkowycz[47]
$l_+ = \kappa y_+$	$\kappa = 0.4$ (planar value)	Ginevdkii & Solodkin[48] Reid & Wilson[3] Bradshaw & Patel[45]
$l_+ = \kappa y_+$	$\kappa = 0.22$ (empirical)	Matsui[27]
$l_+ = \kappa y_+[1 - e^{-(y_+/\lambda_+)}]$	$\kappa = 0.4$ (planar value) $\lambda_+ = 26$ (planar value)	Cebeci[49]
$l_+ = \kappa y_+[\tanh(y_+^2/\lambda_+^2)]^{0.5}$	$\kappa = 0.4$ (planar value) $\lambda_+ = 63/\sqrt{3}$	Patel[50]
Mixing Length Based on Rao Coordinate:		
$l_+ = \kappa\,[a_+\ln(r/a)]\,(r/a)^{0.5}$	$\kappa = 0.4$ (planar value)	White, Lessman & Christoph[51] Rao[42]
$l_+ = \kappa\,[a_+\ln(r/a)]\,[1 - e^{-\{[a_+\ln(r/a)]/\lambda_+\}}]$	$\kappa = 0.4$ (planar value) $\lambda_+ = 26$ (planar value)	Cebeci[52]
$l_+ = \kappa\,[a_+\ln(r/a)]\,[\tanh(y_+^2/\lambda_+^2)]^{0.5}$	$\kappa = 0.4$ (planar value) $\lambda_+ = 63/\sqrt{3}$	Denli & Landweber[8]
Other Cylindrical Mixing Lengths:		
$l_+ = \kappa y_+\,[1 - e^{-(y_+/\lambda_+)}]\,(a/r)^{0.5}$	$\kappa = 0.4$ (planar value) $\lambda_+ = \lambda_+(a_+)$	Granville[53]
$l_+ = (\kappa y_+)\,[r_+/(r_+ + \kappa c y_+)]$	$\kappa = 0.4$ (planar value) $c = 1.5$ (empirical)	Eickhoff[54]
$l_+ = [c\,\delta_+/(dU_+/dy_+)]^{0.5}$	$c = 0.0274$ (empirical)	Lueptow, Leehey & Stellinger[10] Lueptow & Leehey[55]
$l_+ = (\kappa y_+\,[1 + (y_+/2a_+)])\,(a/r)^{1.5}$	$\kappa = 0.4$ (planar value)	Granville[53] based on Richmond[7]

Of course, the application of planar mixing lengths to a cylindrical boundary layer are immediately subject to question. The planar mixing length assumption requires that momentum transfer occur over a length scale that is proportional to the distance from the wall. However, as suggested by Luxton et al.[9] and confirmed using flow visualization by Lueptow and Haritonidis,[31] the scale of flow structures in a cylindrical boundary layer can be much greater than the diameter of the cylinder for small cylinders. In other words, the wall is less likely to control the length scales in a cylindrical boundary layer than in a planar boundary layer. As a result, using a mixing length that is proportional to the distance from the wall is probably inappropriate unless δ/a is small.

Rao[42] used the similarity law (2-5) to derive a mixing length shown in table 2. White, Lessman, and Christoph[51] note that this form of the mixing length, which is smaller than its planar equivalent, is logical since "a cylinder has less ability to create turbulent shear than a plane surface." However, as discussed earlier with regard to equation (2-5), this approach is based on a weak assumption that the wall-normal scaling in the viscous sublayer should carry over to the log region.

A different approach results from the direct substitution of the Rao coordinate, $Y_+ = [a_+ \ln(r/a)]$, for the planar wall-normal coordinate, y_+, in the mixing length scaling. Cebeci[52] repeated his analysis incorporating this substitution in a mixing length with a Van Driest sublayer modification as suggested by White (discussion following reference 49). Denli and Landweber[8] used a mixing length similar to that used by Patel[50] except that the Rao coordinate was used instead of y_+. However, using the Rao coordinate in place of y_+ in the mixing length expression is subject to question for two reasons. First, as noted earlier, the Rao wall-normal coordinate derives from the scaling in the viscous sublayer. Its application to the log region does not necessarily follow. Second, like the planar case, the Rao coordinate-based mixing length is a function of the distance from the wall even though the wall probably has less control over the length scales than in a planar boundary layer.

Two other cylindrical mixing length expressions, noted in table 2, have been proposed. Starting with equation (2-1) and assuming a logarithmic velocity profile, Granville[53] developed an expression for a mixing length that accounts for the transverse curvature of the cylinder. This expression was coupled with the Van Driest sublayer modification noting that the sublayer modification correction coefficient, λ, should be a function of a_+ instead of constant. However the validity of this mixing length may be in doubt, since its derivation depends on the assumption of the existence of a logarithmic relationship between U_+ and y_+. Eickhoff[54] proposed with little justification or rigor that a ratio of radii including an empirical constant should be multiplied times the usual planar mixing length to

include the effect of transverse curvature. This mixing length is based on the weak assumption that as an eddy moves away from the cylinder's wall, a lower velocity fluctuation results in a cylindrical boundary layer than in a planar boundary layer.

Mixing length expressions derived from the similarity laws proposed by Lueptow et al.[10] and Richmond[7] are included to complete table 2.

SIMILARITY LAWS

Similarity laws for the mean velocity profile in the inner region are presented in table 3. As noted earlier, the four similarity laws based on a planar mixing length probably do not appropriately account for the effect of transverse curvature. However, comparison of these similarity laws to experimental data suggests that they show the expected trends for transverse curvature.[11,50]

Three similarity laws included in table 3 are based on Rao's coordinate, $Y_+=[a_+ \ln(r/a)]$. Denli and Landweber[8] used this coordinate in a mixing length to derive a simlarity law. Rao's similarity law[34] is based on the substitution of the sublayer coordinate into the planar log law (equation 2-5). Chase[43] offered a slight modification of this similarity law by adopting a planar term to allow for smooth transition between Rao's sublayer law (equation 2-3) and the similarity law. For reasons outlined earlier, the laws based on a mixing length incorporating Rao's wall-normal coordinate are subject to scrutiny.

The last four similarity laws included in table 3 are not based on mixing length derivations or Rao's wall-normal coordinate. Lueptow et al.[10] proposed a similarity law based on an assumption of constant eddy viscosity in the boundary layer. This results in a log law that is identical to the planar log law, equation (2-4). As mentioned earlier, m and n are dependent upon the ratio δ/a and are empirically determined. The validity of the constant eddy viscosity approach as a first-order approximation was confirmed by direct measurement of the eddy viscosity.[55] Using the method of matched asymptotic expansions, Afzal and Narasimha[58,59] derived an expression for the mean velocity profile that is similar to the planar log law. As a_+ becomes small and δ/a becomes large, the coefficients of the log law are dependent upon these parameters. Thus, the similarity law is very similar to that proposed by Lueptow et al.[10] although the laws were derived using two different approaches.

Table 3. Proposals for Similarity Laws in the Inner Region for a Cylindrical Turbulent Boundary Layer

Log Law	Coefficients	Reference
Planar Mixing Length:		
$U_+ = (1/\kappa)\ \ln(y_+)+B$	$\kappa = 0.4$; $B = 5$	Planar law
$U_+ = (1/\kappa)\ \ln[Q(y/a)/\ Q(y_S/a)]+ a_+\ln[(a+y_S)/a]$	$\kappa = 0.4$	Reid & Wilson[3]
$U_+ = (1/\kappa)\ \ln\{4y_+/[1+(r/a)^{0.5}]^2\}+B$	$\kappa = 0.4$; B function of a_+	Bradshaw & Patel[45]
$U_+ = (1/\kappa)\ \ln[4a_+Q(y/a)]+ B$	$\kappa = 0.4$; B function of a_+	Patel[50]
Mixing Length Based on Rao Coordinate:		
$U_+ = (1/\kappa)\ \ln[a_+(r/a)^{0.5}\ln(r/a)]+B$	$\kappa = 0.4$; B function of a_+	Denli & Landweber[8]
Based on Rao Coordinate:		
$U_+ = A\ \ln[a_+\ln(r/a)]+B$	A,B functions of R_a, a_+	Rao;[34] Rao & Keshavan[11]
$U_+ = (1/\kappa)\ \ln[a_+\ln(r/a)-J]+B$	$\kappa = 0.4$; $J = B = 5$	Chase[43]
Other:		
$U_+ = A\ \ln(y_+)+B$	A,B functions of δ/a	Lueptow, Leehey, & Stellinger[10]
$U_+ = A\ \ln(y_+)+B$	A,B functionsof a_+	Afzal & Narasimha[58,59]
$U_+ = A\ \ln(y_+[1+(y/2a)])+B$	not specified	Richmond[7]
$U_+ = (1/\kappa)\ \ln(y_+)+B$	$\kappa = 0.4$; B function of R_a	Yu[30]

Note: $Q(s)=[\sqrt{(1+s)}-1]/[\sqrt{(1+s)}+1]$; y_S is the thickness of the sublayer.

The similarity laws due to Richmond and Yu are included to complete table 3. As discussed earlier, Richmond's law[7] is unlikely to be useful. The proposal by Yu[30] is based on dimensional arguments and a narrow range of data. Over a broader range of transverse curvature ratios it fails.

2.7 MEAN VELOCITY PROFILE IN THE OUTER REGION

Like a planar boundary layer, the mean velocity profile of a cylindrical boundary layer deviates from a logarithmic profile in its outer region. The mean velocity in the outer region is usually displayed in velocity-defect coordinates, $(U_\infty-U)/U_\tau$ versus y/δ. Willmarth et al.[12] presented velocity-defect profiles over a wide range of transverse curvatures as shown in figure 2. Their data clearly indicate that the velocity profiles do not collapse onto a single curve as they do in the planar case. As the cylinder becomes smaller the velocity-defect profile becomes fuller. As δ/a approaches one, the velocity-defect profiles approach the planar velocity defect profiles. From dimensional arguments Willmarth et al. propose that the velocity defect should be a function of both y/δ and δ/a.

Several outer laws have been proposed for a cylindrical boundary layer as enumerated in table 4. Afzal and Narasimha[58,59] used the method of matched asymptotic expansions to obtain a defect law that is quite similar to the planar outer law except that the multiplicative coefficient is dependent upon a_+ and the additive coefficient is a function of both δ/a and a_+. Of course, the coefficients approach the planar values as the effect of transverse curvature diminishes [$\delta/a = O(1)$ and a_+ very large]. Yu[30] developed an outer law based on a length scale dependent upon the friction velocity and the kinematic viscosity. Although experimental data were shown to collapse onto a single curve, the range of transverse curvature ratios is very small, so no conclusions can be drawn. Based on similarity to an axisymmetric wake, Rao and Keshevan[11] proposed plotting the velocity defect versus $r_+=(a+y)U_\tau/\nu$. Denli and Landweber[8] used a mean-flow equation simplified by using the free stream velocity in the convective term (Oseen's approximation) and an eddy viscosity model that is a function of the longitudinal coordinate for the shear stress in the outer layer to derive a complex outer law requiring six empirical constants. The resulting velocity profiles match the data of Willmarth et al.[12] for δ/a ranging from 2 to 16. Adomaitis[36] developed an outer law based on the planar outer law and using Rao's coordinates and replacing δ with the displacement thickness, δ_*. This formulation appears adequate for

a narrow range of δ/a. Adornaitis also documented the effect of free stream turbulence on the boundary layer profile.

Like a planar boundary layer, the deviation of the velocity profile in the outer layer is thought of in terms of a modification of the logarithmic velocity profile known as a wake law. Rao and Keshavan[11] identified two versions of a wake component in a cylindrical boundary layer. The wake is termed "negative" if the boundary layer profile drops below the log law as the distance from the wall increases and "positive" if the boundary layer profile rises above the log law. The positive wake's appearance is similar to a planar wake. Although Rao and Keshavan considered a log law of the form of (2-5), these wakes are observed regardless whether the data are plotted as a function of the planar wall-normal coordinate or Rao's wall-normal coordinate.

For minimal transverse curvature ($\delta/a<2$), the wake is positive and the appearance of the mean velocity profile is nearly identical to the planar profile.[32,37,39-41] Chin et al.[37] proposed a wake law that is very similar to the planar wake law (see table 4). For slightly larger curvature ratios [$\delta/a=O(2)$] the positive wake is not evident.[14,36] Rao and Keshavan[11] found that as the boundary layer developed, the wake went from negative to positive at a given R_a. They went on to propose that the radial coordinate at which the velocity profile deviates from the logarithmic profile is dependent upon R_a. Their explanation of this phenomenon involves the relationship between the outer portion of an axisymmetric boundary layer and properties of an axisymmetric wake.

On the other hand Afzal and Narasimha[58] call existence of these wakes into question by proposing that the flows where they exist may not be fully developed. The data of Willmarth et al.[12] spans a wide range of transverse curvatures and shows a positive wake for large transverse curvature ($\delta/a<5$) and a slight tendency toward a negative wake as the transverse curvature decreases ($\delta/a>9$). However they point out that the negative wake in a cylindrical boundary layer is not as obvious as the positive wake in the planar case, in spite of the expectation that a cylindrical boundary layer should be more wake-like than a planar boundary layer. As a result, the existence of a wake region in a cylindrical boundary remains unclear.

Table 4. Proposals for Outer Laws for a Cylindrical Boundary Layer

Outer Law	Coefficients	Reference
$(U_\infty - U)/U_\tau = (-1/\kappa)\ln(y/\delta)+C$	κ=0.4; C =2.5	Planar law
$(U_\infty - U)/U_\tau = -A\ln(y/\delta)+C$	A function of a_+; C function of $\delta/a, a_+$	Afzal & Narasimha[58,59]
$(U_\infty - U)/U_\tau = (-1/\kappa)\ln[y_+\exp(-U_\infty/\kappa U_\tau)]+C$	κ=0.4; C function of R_a	Yu[30]
$(U_\infty - U)/U_\tau = -A\ln(r_+)+C$	A,C functions of R_a	Rao & Keshavan[11]
$(U_\infty - U)/U_\infty = f[R_a, x/aR_a, r/(\delta+a)]$		Denli & Landweber[6]
$(U_\infty - U)/U_\tau = (-1/\kappa)\ln\{[a U_\tau \ln(r/a)]/(U_\infty \delta_x)\}+C$	κ=0.4; C function of δ/a	Adomaitis[36]
$(U_\infty - U)/U_\tau = -A\ln(y/\delta)+C(1-\cos(\pi y/\delta))$	A =1.95; C = 0.9	Chin, Hulsebos, & Hunnicutt[37]

2.8 RESULTS OF ANALYTIC MODELS OF A CYLINDRICAL BOUNDARY LAYER

Several models of a cylindrical boundary layer have been used to evaluate the effect of transverse curvature on characteristics of a boundary layer such as the coefficient of friction, the momentum thickness and the displacement thickness. The procedure begins with the development of a mean velocity profile based on one of the mixing length closure schemes described earlier or based on the assumption of a particular form for the mean velocity profile. From the velocity profile the coefficient of friction, C_f, can be evaluated from the momentum integral, i.e.,[15]

$$\frac{C_f}{2} = \left(\frac{U_\tau}{U_\infty}\right)^2 = \frac{d}{dx}\int_a^{a+\delta}\left[\frac{U}{U_\infty}\left(1-\frac{U}{U_\infty}\right)\left(\frac{r}{a}\right)\right]dr. \qquad (2\text{-}7)$$

The model mean velocity profile can also be used to evaluate the integral thicknesses. The definitions for the integral thicknesses differ from those for a planar boundary layer because of the effect of transverse curvature.[60] The displacement thickness, δ_*, and the momentum thickness, θ, are given by equations (2-8) and (2-9), respectively.

$$\delta_* \left[1 + (\delta_*/2a)\right] = \int_a^{a+\delta} \left[\left(1 - \frac{u}{U_\infty}\right) \left(\frac{r}{a}\right)\right] dr, \tag{2-8}$$

$$\theta \left[1 + (\theta/2a)\right] = \int_a^{a+\delta} \left[\frac{u}{U_\infty} \left(1 - \frac{u}{U_\infty}\right) \left(\frac{r}{a}\right)\right] dr. \tag{2-9}$$

Table 5 indicates the functional dependence of the coefficient of friction and the integral thicknesses predicted using various models of the cylindrical boundary layer. The analyses are grouped according the model used for the mean velocity profile. The table also indicates if representative mean velocity profiles were presented and if they were compared to experimental results.

The earliest attempts to model a cylindrical boundary layer used a power law formulation for the mean velocity profile. Millikan,[61]* Landweber,[62] Eckert,[2] and Sakiadis[4] used a 1/7-power law formulation assuming similarity to a planar boundary layer. Karha [70] and Liu and Dai[63] varied the exponent of the power law in attempts to refine the mean velocity profile to account for transverse curvature. The power law description of the boundary layer profile predicts that transverse curvature will increase the skin friction compared to the planar case. However, because of the crudeness of the velocity profile models, the predictions are not quantitatively correct.

The analytic models based on the planar mixing length are automatically subject to scrutiny because of the premise of similarity of the mixing length in the cylindrical case to the mixing length in the planar case. In spite of this weakness, the analyses of Sparrow et al.[47] and Cebeci[49] stand out for their

---

* Millikan's model was the first of several that have been based on momentum integral methods. While these methods have generated considerable interest,[69] a necessary assumption for their application is that $\delta \ll a$. Since this report is generally concerned with situations where $\delta \geq a$, discussion of these methods is omitted.

estimates of the skin friction over a wide range of cylinder diameters, R_a, and axial positions, R_x. These results indicate that the coefficient of friction decreases with increasing R_a and R_x. Sparrow et al. explained this in the following way: "... the difference in the flow field about a cylinder and that about a flat plate is due to the expansion in flow area encountered with increasing distance from the cylindrical surface. When the boundary layer is very thin relative to the cylinder radius, then there is a correspondingly small area change across the boundary layer, and the cylinder behaves like a flat plate. On the other hand, when the boundary layer is thick compared with the cylinder radius, there is a substantial area change and a larger difference between flat plate and cylinder... Therefore, the larger the length Reynolds number Re_x [R_x], the thicker the boundary layer and the greater the effect of cylindrical geometry. The cylinder Reynolds number Re_{r0} [R_a] is a direct measure of the radius of the cylinder and so, the smaller the Re_{r0} [R_a], the greater the curvature effect."

In spite of use of a planar mixing length model in these analyses, the results show characteristics that correspond to experimental results. Representative velocity profiles presented by Sparrow et al. show the shallow slope of the log region of the mean velocity profile as the cylinder radius becomes small. The log regions of their velocity profiles also show a slight downward curvature that is also vaguely evident in the experimental data of Willmarth et al.[12] for very small cylinders. A similar trend is seen in the representative velocity profiles presented by Patel.[50]

Using planar mixing length closure models, Reid and Wilson[3] and Matsui[27] found the unlikely result that the average skin friction is a function of R_a alone with no dependence upon the length of the cylinder. Ginevskii and Solodkin[48] show qualitatively similar results over a narrower range of parameters. Reid and Wilson also considered the effect of wall roughness on the skin friction.

The use of cylindrical mixing length models noted in table 5 would be expected to provide a more appropriate model compared to the planar mixing length models. Although several of the authors who used this type of analysis compare their mean velocity profile to experimental data, only Denli and Landweber[8] go so far as to calculate the skin friction and the integral thicknesses. Their calculations agree with the experimental results of Willmarth et al.,[12] although this may be a result of the use of this experimental data to determine the empirical coefficients used in the analysis.

Table 5: Functional Dependence of the Coefficient of Friction and the Integral Thicknesses for a Cylindrical Boundary Layer

Reference	Mean Velocity Profile[a]	Coefficient of Friction[b]	Integral Thickness[b]	Notes
Power Law:				
Millikan[61]	-	R_V	R_V, x	R_V based on volume
Eckert[2]	-	δ/a	δ/a	compressible
Liu & Dai[63]	-	x	x	-
Sakiadis[4]	-	-	ξ	-
Planar Mixing Length Closure:				
Cebeci[49]	comparison	R_a, R_x	-	heat transfer
Ginevskii & Solodkin[48]	sample prof.	x/a, R_a	δ/a	-
Matsui[27]	-	R_a	-	extruding
Patel[50]	comparison	-	-	-
Reid & Wilson[3]	sample prof.	R_a	-	roughness
Sparrow et al.[47]	sample prof.	R_a, R_x	-	heat transfer
Cylindrical Mixing Length Closure:				
Cebeci[52]	comparison	-	-	-
Donli & Landweber[8]	comparison	-	ξ	-
Eickhoff[54]	comparison	-	-	-
Granville[53]	-	-	-	kinetic energy
Rao[34]	comparison	-	-	-
Assumed Velocity Profile:				
Ackroyd[64]	-	R_a, R_x	-	extruding
White[65]	comparison	R_a, R_x	x/a, R_x	-
White et al.[51]	-	R_a, R_x	-	compressible
Other Methods:				
Abdelhalim et al.[66]	-	-	-	-
Shanebrook & Sumner[67]	comparison	-	x	-
Yu[30]	comparison	R_a, δ/a	R_a, δ/a	-

Notes:

a) "Comparison" means that the mean velocity profile was compared to experimental data. "Sample prof." means that sample mean velocity profiles were provided but not compared to experiments.

b) Parameters shown indicate the functional dependence of the coefficient of friction or the integral thicknesses (displacement, momentum, or boundary layer) that is predicted by the analysis.

Other approaches based on assuming a velocity profile instead of using a mixing length have been used for analysis of cylindrical boundary layer. White[65] substituted Rao's wall-normal coordinate in place of y_1 in Spalding's expression[71] for the velocity profile in a planar boundary layer. Ackroyd[64] corrected errors in White's analysis and followed a similar approach for the problem of an extruding cylinder. The results for a cylinder in a uniform stream and for an extruding cylinder are very similar. Both White and Ackroyd present results over a wide range of parameters showing that the coefficient of friction decreases with increasing R_a and R_x (see figure 4). Unfortunately, the analysis is dependent upon the presumed similarity of Spalding's mean velocity profile using the Rao coordinate with the velocity profile in a cylindrical boundary layer. Although Ackroyd clearly shows that the assumed profile is quite different from experimental data for large δ/a, his results are shown in figure 4 since they show the trends also found by several other researchers.[47,49] White et al.[51] carried the analysis further to include compressibility.

Finally, three other methods of modeling a cylindrical boundary layer were used. An entrainment theory based on the momentum equation and an entrainment equation derived from continuity was adapted by Shanebrook and Sumner[67] for application to axisymmetric boundary layers. Granville[68] extended this work substantially by incorporating more sophisticated shape parameter functions and velocity profiles. Yu[30] developed a log law and an outer law similar to those for a flat plate and used these laws to predict the boundary layer thickness development and the skin friction for cylinders with large R_a. Abdelhalim et al.[66] developed a method for analyzing the flow past semi-infinite axisymmetric and planar bodies with a blunt leading edge condition using conformal coordinates and the k-ε turbulence model (a two-equation closure scheme). Although results were presented for the planar case, the equations were not solved for an axisymmetric boundary layer.

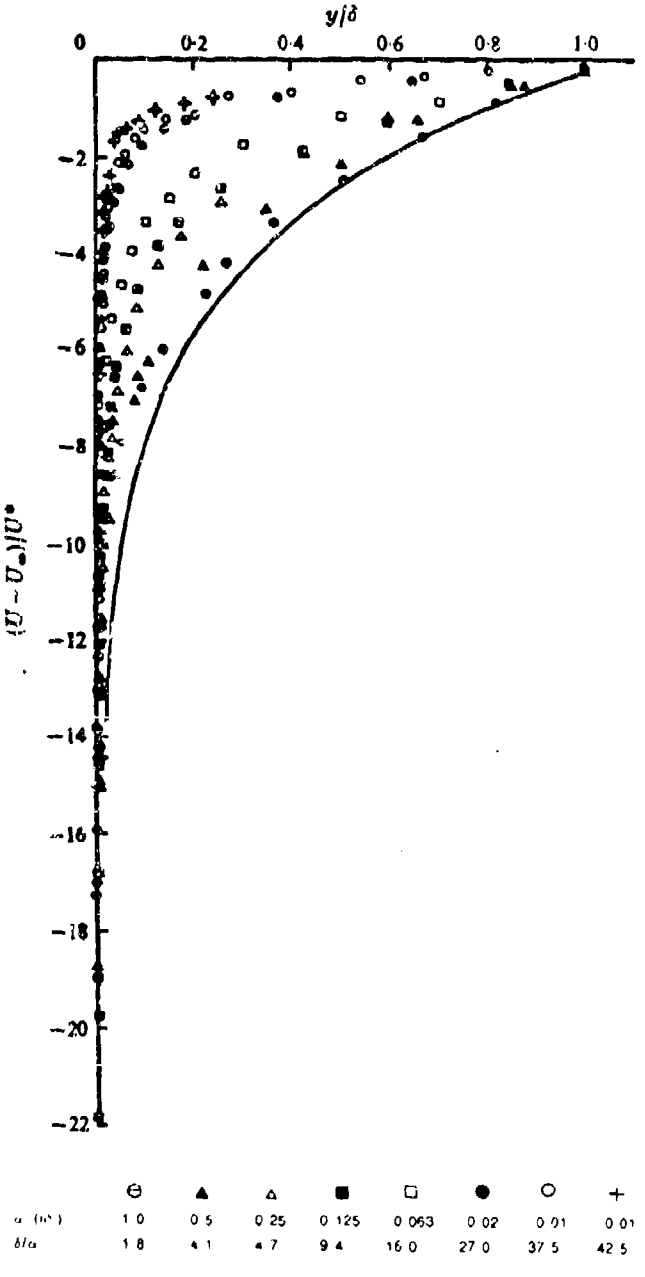

Figure 2. Representative Velocity -Defect Profiles Showing the Influence of Transverse Curvature [Willmarth et al.[12] ——— Flat plate.[13] (U_* is the friction velocity.)

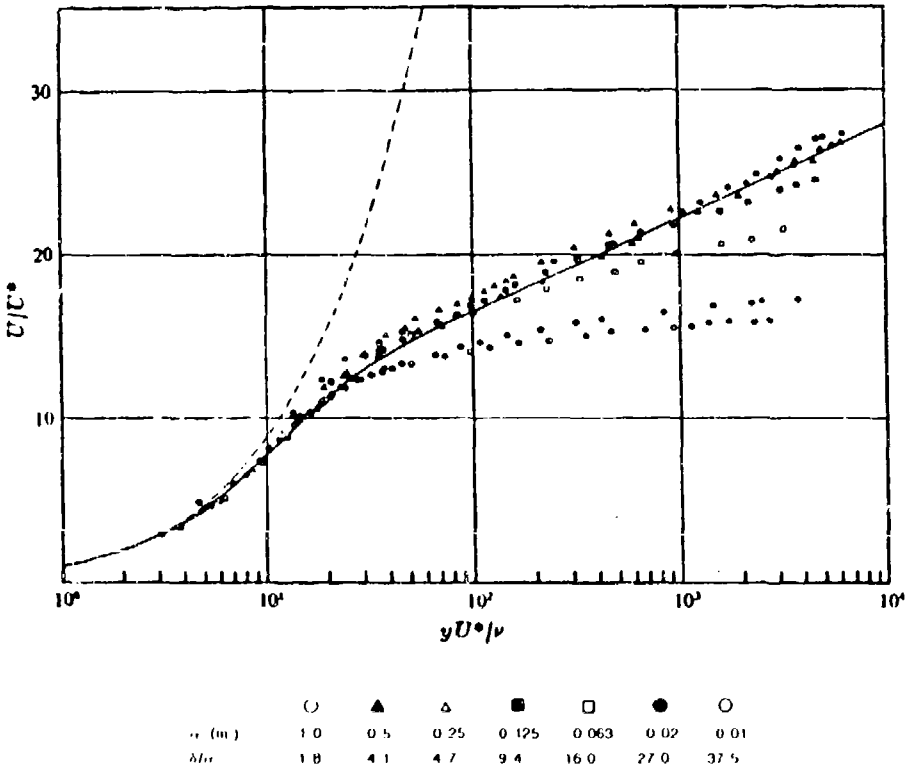

Figure 3. Representative Velocity Profiles in Wall Coordinates Showing the Influence of Transverse Curvature

[Willmarth et al.[12] ——— Flat plate;[16] - - - - - - Sublayer mean velocity profile (equation 2-3 with a_+=33.4). (U_* is the friction velocity.) Reprinted with the permission of Cambridge University Press, copynght 1976.]

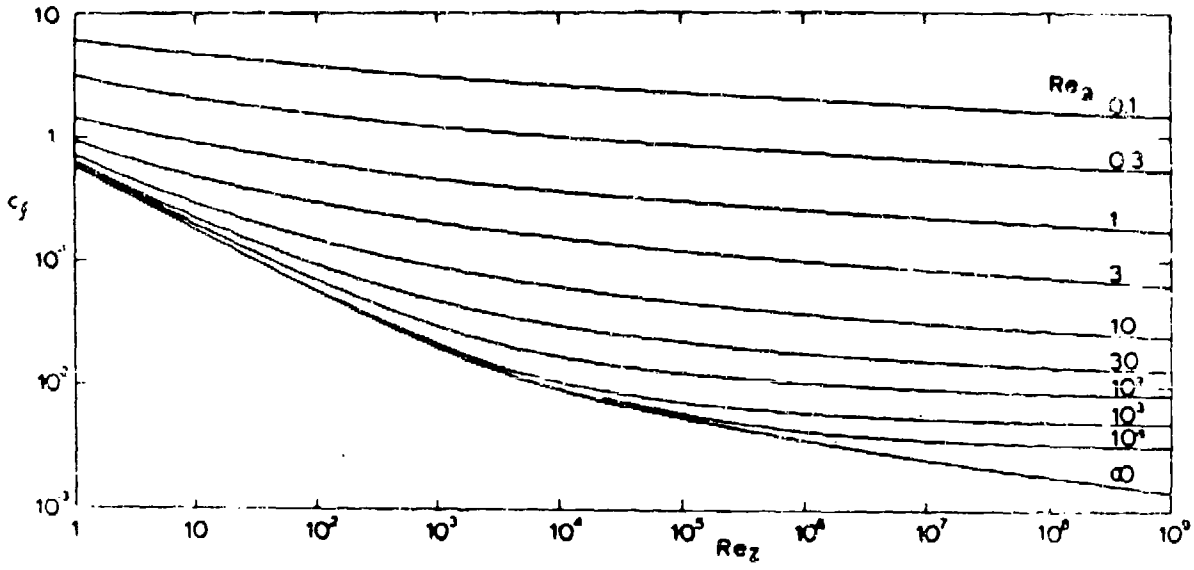

Figure 4. Coefficient of Friction on a Cylinder in a Uniform Axial Flow

[Ackroyd[64] ($Re_a = R_a$; $Re_z = R_x$) . Reprinted with the permission of the ASME, copyright 1982.]

3. TURBULENCE IN A CYLINDRICAL BOUNDARY LAYER

Although the emphasis in research on cylindrical boundary layers has centered on the measurement and analysis of the mean velocity profile, some experimental work has been done on the turbulent character of a cylindrical boundary layer. Most of the research has centered on the measurement of turbulence in a cylindrical boundary layer and the comparison of these measurements with a planar boundary layer.

3.1 REYNOLDS STRESS

Surprisingly few measurements of the Reynolds stress, $\overline{uv}$, have been made in a cylindrical boundary layer. Measurements of the velocity fluctuations are difficult for two reasons. First, the measurement of the wall-normal fluctuations requires the use of X- or V-shaped hot wire probes that are difficult to calibrate and use. Second, since the wall-normal gradients are large, the measured wall-normal velocity is strongly affected by the averaging of the velocity over the wall-normal dimension of the hot-wire.

The Reynolds stress profile in a cylindrical boundary layer is very similar to that in a planar boundary layer when the effects of curvature are small, $\delta/a<2$.[32,41,72] As δ/a gets large, though, the Reynolds stress profile becomes quite different from that of a flat plate as shown in figure 5.[10] The Reynolds stress drops off much more quickly with distance from the wall in a cylindrical boundary layer than in a planar boundary layer. Lueptow et al. attribute this to the cylindrical geometry.[10] From equation (2-1) and (2-2) they suggest that the Reynolds stress should be a function of 1/r. Plots of the Reynolds stress nondimensionalized with the free-stream velocity versus a/r appear to result in weak collapse of the data onto a single curve that may be considered to be a straight line as a first approximation. Assuming inertial effects are small throughout the boundary layer, equation (2-1) suggests that the slope of this line is equal to the coefficient of friction. Using this method underestimates the wall shear stress, but the degree of agreement of the estimates of the coefficient of friction with that of other methods is quite surprising considering the necessary assumptions.[31]

The Reynolds stress nondimensionalized with u_{rms} and v_{rms}, where $u_{rms} = \sqrt{\overline{(uu)}}$, is nearly constant across the entire boundary layer, except near the wall and near the outer edge of the boundary

layer where it necessarily drops off.[10,32] Like a planar boundary layer the value of $\overline{uv}/(u_{rms}v_{rms}) \approx 0.5$ throughout most of the boundary layer.

3.2 TURBULENT KINETIC ENERGY

The kinetic energy of the turbulent velocity fluctuations is given by

$$E_k = (1/2)\,\rho\,\overline{u_i u_i} = (1/2)\,\rho\,(\overline{uu} + \overline{vv} + \overline{ww}), \qquad (3\text{-}1)$$

where u, v, and w are the velocity fluctuations in the streamwise, wall-normal, and spanwise directions, respectively. Like the measurement of the wall-normal velocity fluctuations, the measurement of the spanwise fluctuations is difficult.

The velocity fluctuations in a cylindrical boundary layer are nearly identical to the measurements of these quantities in a planar boundary layer for $\delta/a<1$.[41,72] For larger values of δ/a the streamwise velocity fluctuations, which are the largest contributor to the turbulent kinetic energy, appear to drop off more quickly with distance from the wall than the planar case.[32] On the other hand, the general character of the streamwise and wall-normal velocity fluctuations near the wall is similar to that of a flat plate as shown in figure 6.[31] The data indicates Reynolds number similarity near the wall when the streamwise velocity fluctuations nondimensionalized by the friction velocity are plotted as a function of y_+. The streamwise velocity fluctuations rise quickly from zero at the wall reaching a maximum value of $u_{rms}/U_\tau = 3.2$ at $y+ \approx 13$ and dropping off gradually with distance from the wall from that point to the outer edge of the boundary layer. Luxton et al.[9] and Lueptow et al.[10] measured a slightly smaller maximum value of u_{rms}/U_τ, although the discrepancy may be related to probe resolution and measurement techniques. The wall-normal fluctuations reach a maximum value of $v_{rms}/U_\tau \approx 1$. The maximum velocity fluctuations and the distance from the wall where they occur are similar to channel flow and planar boundary layer flow. The similarity between the distribution of the streamwise and wall-normal velocity fluctuations in a cylindrical boundary layer and other wall-bounded flows suggests that the mechanism for the generation of the turbulence at the wall may be the same.

Adomaitis[36] found that the magnitude of streamwise velocity fluctuations increase even very close to the wall when the free stream turbulence intensity increases. No measurements of the spanwise velocity fluctuations have been made for $\delta/a>1$.

3.3 HIGHER ORDER VELOCITY STATISTICS

The streamwise skewness, $\overline{u^3}/u_{rms}^3$, is a measure of the direction of excursions from the mean (positive excursions imply positive skewness, negative excursions imply negative skewness, and a Gaussian distribution has zero skewness). The skewness in a cylindrical boundary layer is similar to that of other wall-bounded flows with a value between 0 and -1 through most of the boundary layer.[9,74] Near the wall the streamwise skewness becomes positive suggesting the presence of sweep structures subsequent to a burst (see section 4). In the outer part of the boundary layer the skewness becomes more negative because of the intermittency of the turbulence. The wall-normal skewness is slightly positive throughout the boundary layer[74] indicating that the largest excursions from the mean are positive. This may be related to the liftup of a burst near the wall and the mild positive wall-normal flow in the intermittent region near the edge of the boundary layer.

The streamwise flatness, $\overline{u^4}/u_{rms}^4$, is a measure of the magnitude of excursions from the mean (a Gaussian distribution has a flatness of 3; flatness greater than 3 indicates a probability distribution with long tails; flatness less than 3 indicates a probability distribution with short tails). The streamwise and wall-normal flatness are nearly Gaussian throughout most of the boundary layer. Near the wall the flatness is greater than 3, probably because of the burst-sweep cycle. In the outer portion of the boundary layer the flatness is greater than 3 as a result of intermittency.[9,74]

3.4 VELOCITY SPECTRA AND AUTOCORRELATIONS

The spectrum of the streamwise velocity fluctuations is indicative of the energy content of the velocity fluctuations at a particular frequency, f. For small δ/a the spectra appear to be similar in character to the planar streamwise velocity spectra,[32,41] although it is difficult to make direct comparisons because of different scaling techniques. Some data suggest that the energy in a cylindrical boundary layer is shifted to higher frequencies compared to a planar boundary layer.[32]

Lueptow and Haritonidis[31] presented the energy density function, E, of the velocity fluctuations such that the area under the spectrum for a given frequency range is equivalent to the turbulent energy in that frequency range. The ordinate is normalized so that the total area under the curve is 1, i.e.,

$$\int_0^{\infty} (fE/U_{rms}^2)\ d(\ln f) = 1. \qquad (3\text{-}2)$$

This format allows the easy identification of the frequency range that has the largest contribution to the turbulent energy. Using this format, Lueptow and Haritonidis found that the maximum energy content of the velocity fluctuations occurs in the same frequency band regardless of distance from the wall for $\delta/a \approx 7$ as indicated in figure 7. This suggests that turbulent eddies are about the same size regardless of the distance from the wall supporting a constant eddy viscosity model for the turbulent shear stresses.

Lueptow and Haritonidis[31] found that an outer scaling for the frequency, $f_0 = f\delta/U_\infty$, results in a better collapse of streamwise velocity spectra for different Reynolds numbers than an inner scaling, $f_+ = fv/U_\tau^2$, especially at low frequencies as shown in figure 8. Very near the wall, $y+<10$, they found that an inner scaling worked best. On the other hand, Luxton et al.[9] found no Reynolds number similarity when the spectra are scaled using the outer scales of the momentum thickness and U_∞. As shown in figure 8, the energy content of the wall-normal velocity fluctuations is substantially less than the streamwise velocity fluctuations and the maximum energy density occurs at a higher frequency.[31] The two spectra merge at high frequencies.

The streamwise velocity autocorrelation indicates that the turbulent integral length scales in the outer portion of a cylindrical boundary layer are less than half the size of the length scales in a planar boundary layer.[32] The data of Luxton et al.[9] suggest that length scales derived from the autocorrelation appear to be slightly dependent upon the location in the boundary layer. They are about twice as large at $y_+ = 540$ than they are at $y_+ = 10$ for $\delta/a \approx 27$. Comparing these two studies it appears that the length scales, L, are much larger for large δ/a. At $y/\delta \approx 0.5$, the autocorrelation falls to 1/e at $L \approx 0.08\delta$ for $\delta/a = 1.6$, but the equivalent value is $L \approx 0.8\delta$ for $\delta/a = 27$. This suggests that the influence of the wall on integral length scales is minor for large δ/a.

3.5 WALL PRESSURE

The wall pressure spectrum, autocorrelation and convection velocity for boundary layers with slight transverse curvature ($\delta/a<0.1$) are in agreement with data obtained for planar boundary layers and pipe flow.[75,76] For larger δ/a, Willmarth and Yang[14] and Willmarth et al.[12] investigated the wall pressure fluctuations using an array of 0.06-inch (0.15 cm) flush-mounted piezoelectric pressure transducers on a 3-inch (7.6 cm) diameter cylinder ($\delta/a \approx 2$) and on a 1-inch (2.5 cm) diameter cylinder ($\delta/a \approx 4$). The convection velocity of wall pressure fluctuations derived from the space-time wall pressure correlation was

found to be nearly the same as that for a planar boundary layer increasing with streamwise separation from $0.6U_\infty$ to $0.8U_\infty$. However, since the mean velocity profile convecting the eddies is fuller because of the transverse curvature, the turbulent eddies must be smaller to result in the same convection velocity as in a planar boundary layer. Consistent with this idea, the power spectra of the wall pressure fluctuations for a cylindrical boundary layer contain a greater energy density at higher frequencies than a planar boundary layer as shown in figure 9.

Constant wall pressure correlation contours in a cylindrical boundary layer are nearly circular in the streamwise-spanwise plane.[14] This is in contrast to the elongation of the contours in the spanwise direction measured in a flat plate boundary layer as shown in figure 10. Willmarth and Yang suggest the following explanation. Consider a large eddy adjacent to the curved wall of a cylinder. The mean velocity at the spanwise sides of the eddy is necessarily larger in a cylindrical boundary layer than in a planar boundary layer, since the distance from the wall to the side of the eddy is greater. This results in a shearing motion on the sides of the eddy and reduces its transverse scale. However, the data of Willmarth et al.[12] confuses the issue somewhat. They measured wall pressure contours for $\delta/a\approx4$ that were more elongated in the spanwise direction than measured by Willmarth and Yang for $\delta/a\approx2$ but less than in the planar case ($\delta/a=0$).

The difference in the wall pressure correlation contours between a cylindrical boundary layer and a planar boundary layer suggest differences in the wavenumber spectra of the wall pressure for the two cases. As noted by Blake[80] with regard to the expression for the wavenumber spectrum of the mean-shear-turbulence interaction term, the spectrum of pressure fluctuations in the streamwise direction is enhanced relative to the spanwise direction in the planar case. This results in spatial pressure correlations that reflect smaller scales in the streamwise direction than in the spanwise direction. The larger scales in the spanwise direction are evident in the elongation of the contours in the spanwise direction. Although, an extension of this approach to a cylindrical boundary layer is beyond the scope of this work, it seems likely that the differences in the wall pressure correlation contours displayed in figure 10 are related to differences in the wavenumber spectra for the wall pressure.

Two analyses related to the low-wavenumber spectrum of the wall pressure have been undertaken. Chase and Noiseux[81] related the turbulent wall pressure fluctuations in a cylindrical boundary layer to nonlinear fluctuating velocity products, or Reynolds stress sources. Using a perturbation approach they derived integral relations expressing the wall pressure amplitude at a given wavenumber and frequency as an integral over the nonlinear sources. The expressions were developed for the low-wavenumber domain as expansions in a parameter $U_\infty k/\omega \ll 1$, where k is the streamwise

wavenumber and ω is the angular frequency. Although this work provides a analytic framework, its extension requires the modeling of the source spectra. Dhanak[82] investigated the low-wavenumber domain of pressure fluctuations in a cylindrical boundary layer for $\delta/a \ll 1$. Beginning with the Lighthill formulation in cylindrical coordinates, the low-wavenumber approximation to spectral density was found in terms of a product of source terms and a response function related to the cylindrical geometry. Unknown functions of frequency appearing in the analysis will need to be determined experimentally to advance this work.

Willmarth et al.[33] investigated the wall pressure on cylinder subject to slight cross-flow. For a yaw angle of 2.4° they found that the root-mean-square wall pressure is 15% higher on the windward side and 35% lower on the leeward side than on a cylinder with zero yaw. The windward side wall pressure contained more energy in the high frequency components than the leeward side. Interestingly, periodic oscillations of the wall pressure were not detected indicating an absence of vortex shedding for small yaw angles.

3.6 FLUCTUATING WALL SHEAR STRESS

The fluctuating wall shear stress has not been measured for a cylindrical boundary layer. This is largely due to the difficulty in the application of the usual methods for the measurement of wall shear stress to small cylinders.

3.7 INTERMITTENCY

The intermittency at the outer edge of a cylindrical boundary layer was measured by Lueptow and Haritonidis[31] for $\delta/a=7$. Using a detection scheme based on the square of the first derivative of the velocity, they found that the instantaneous location of the interface between turbulent and non-turbulent flow is Gaussian in character just like a planar boundary layer and that the data collapse onto a single curve for several Reynolds numbers. However, the mean location of the interface was at $y/\delta=1.0$ compared with $y/\delta=0.8$ for a flat plate boundary layer. They attribute this difference to more energetic streamwise velocity fluctuations further out in a cylindrical boundary layer than in a planar boundary layer and to the "filling out" of the boundary layer with turbulent eddies since the cylinder does not constrain the motion of the eddies like a flat plate does.

3.8 RELAMINARIZATION

Substantial discussion regarding the relaminarization of a turbulent cylindrical boundary layer has resulted from consideration of extremely small cylinders where $\delta/a \rightarrow \infty$ and $R_a \rightarrow 0$. Cebeci[40] tried to relate the minimum Reynolds number based on momentum thickness that is a necessary, though not sufficient, condition for turbulence to this problem. For R_a=10, he predicted that the displacement thickness would need to be at least 32 times greater than the cylinder radius for the flow to remain turbulent. Based on extrapolation of their experimental results, Rao and Keshavan[11] proposed that relaminarization may occur when R_a =15,000 because the coefficient of friction for laminar flow will match that for turbulent flow very far downstream. This critical Reynolds number is close to the value of R_a=11,000 below which small disturbance will be damped based on hydrodynamic stability of a cylindrical boundary layer.[83] White[65] argued that similar coefficients of friction for laminar and turbulent flow suggest relaminarization at R_a=3. Turbulent cylindrical boundary layers have been measured for R_a as small as 96 and 140.[7,9]

Patel[50] pointed to "the rather remarkable similarity between the influence of a favourable pressure gradient and that of transverse wall curvature." Using a shear stress gradient parameter related to relaminarization in a planar boundary layer with a favorable pressure gradient, he predicted that a cylindrical boundary layer would relaminarize for a_+<28. Afzal and Narasimha[58] supported this proposal based upon the "inadequate energy supply from the surface [wall]." However, Willmarth et al.[12] pointed out that the apparent similarity in the mean velocity profiles for a cylindrical boundary layer and a planar boundary layer with a favorable pressure gradient result from quite different physical phenomena. Transverse curvature causes a full velocity profile in a cylindrical boundary layer whereas free stream acceleration causes the same effect in a planar boundary layer with a favorable pressure gradient. In any case Luxton et al.[9] measured turbulent flow on a cylinder for a_+ as small as 13.

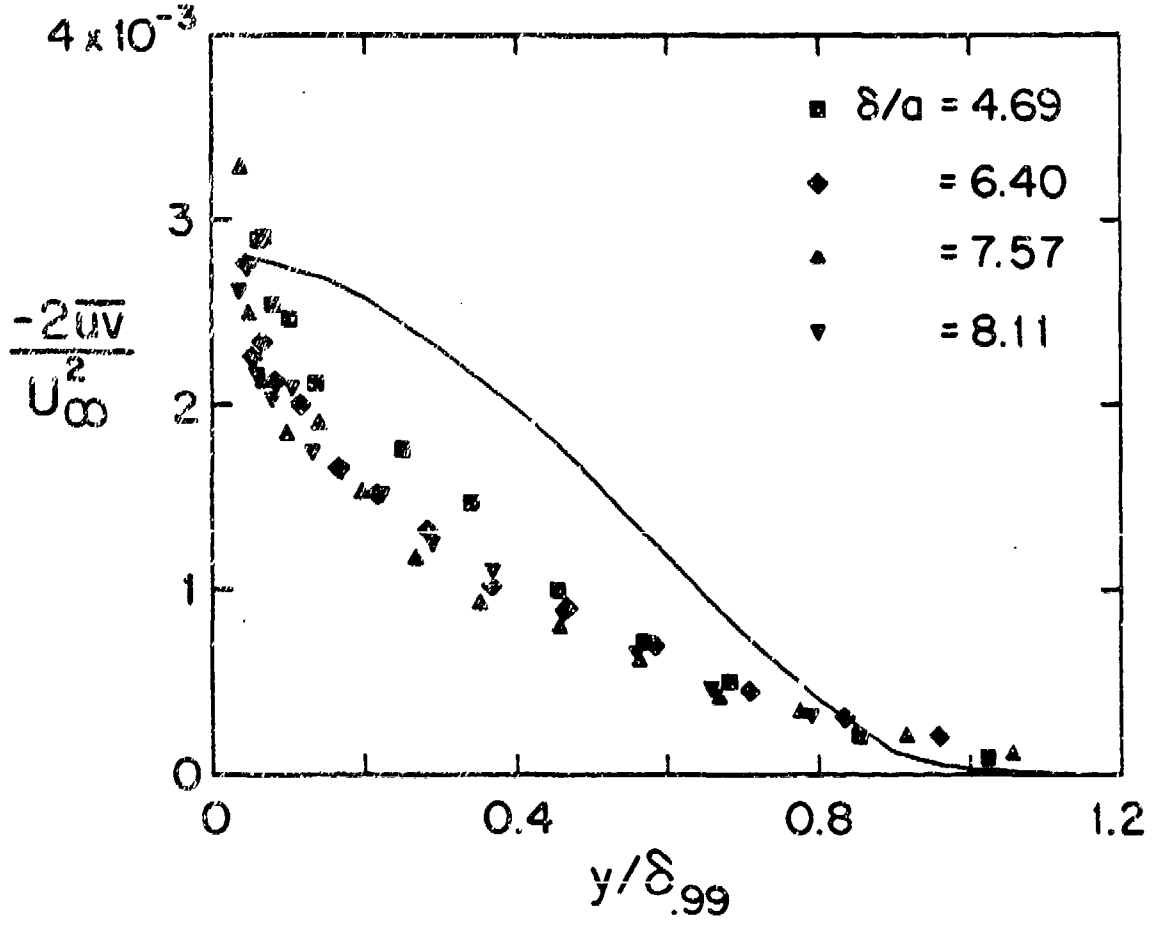

Figure 5. Profile of the Reynolds Stress in a Cylindrical Boundary Layer [Lueptow et al.[10] ——— Flat plate.[73] Reprinted with the permission of the American Institute of Physics, copyright 1985.]

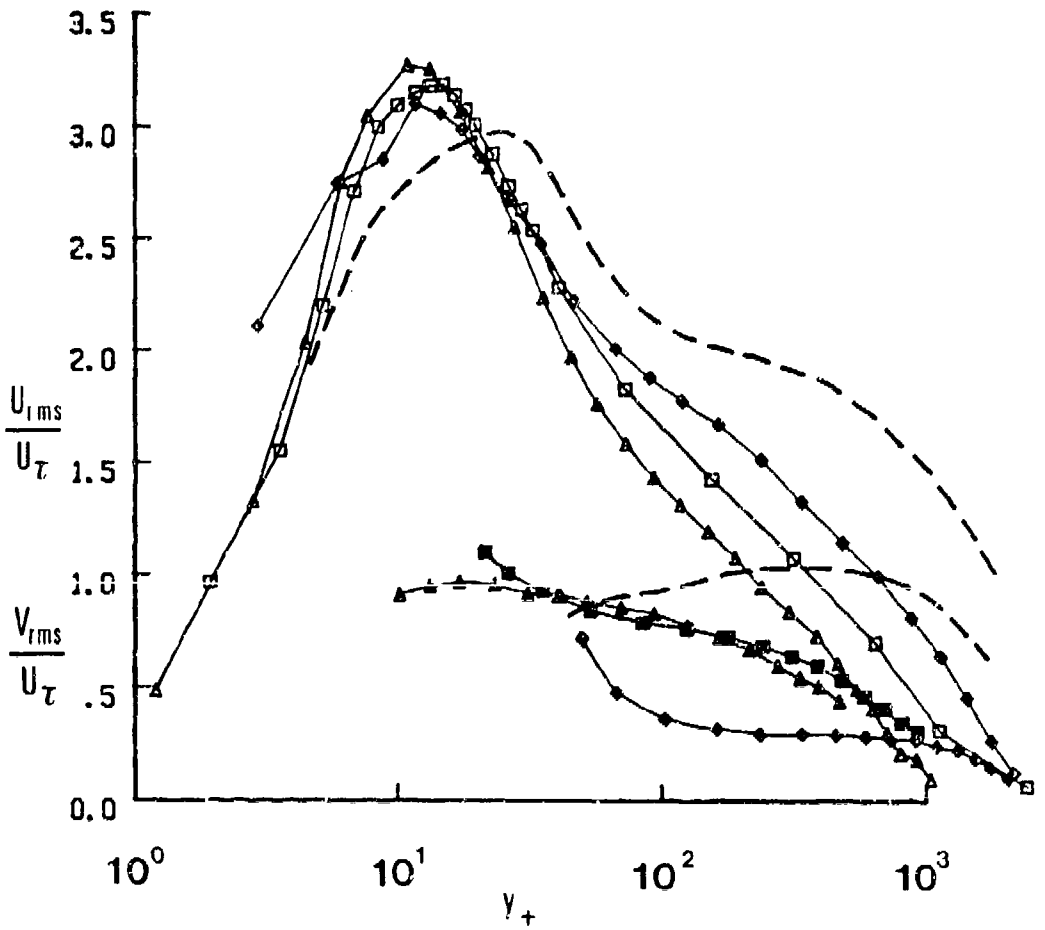

Figure 6. Profile of the Streamwise (open symbols) and Wall-Normal Turbulence Intensity (filled symbols) in a Cylindrical Boundary Layer
[Lueptow and Haritonidis.[31] Δ $R_\theta \approx 2000$; [] $R_\theta \approx 3300$; ◇$R_\theta \approx 5600$. - - - - Flat plat [71]

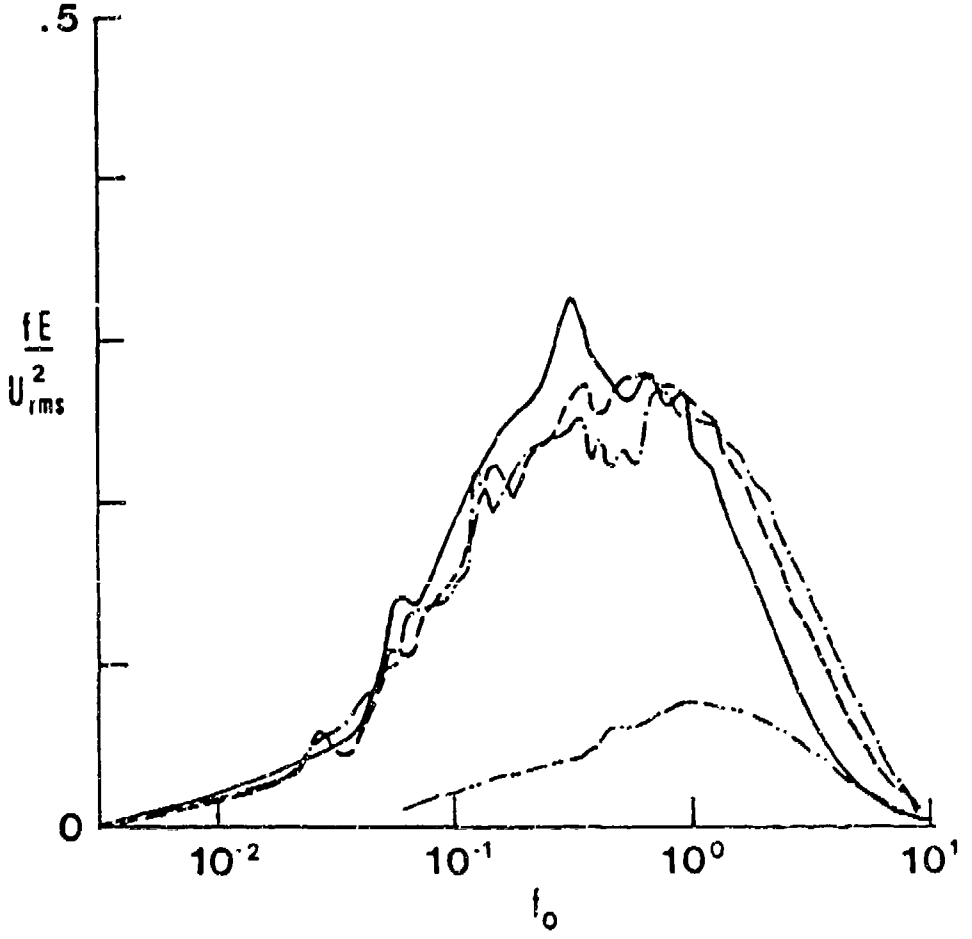

Figure 7. Streamwise and Wall-Normal Velocity Spectra Near the Wall in a Cylindrical Boundary Layer: —— $R_\theta \approx 2000$, $y_+ \approx 37$; - - - - $R_\theta \approx 3300$, $y_+ \approx 32$; - · - · - · $R_\theta \approx 5600$, $y_+ \approx 47$. Wall-Normal Velocity Spectra: - ·· - ·· - ·· $R_\theta \approx 2000$, $y_+ \approx 37$ [Lueptow and Haritonidis.[31] Reprinted with the permission of the American Institute of Physics, copyright 1987.]

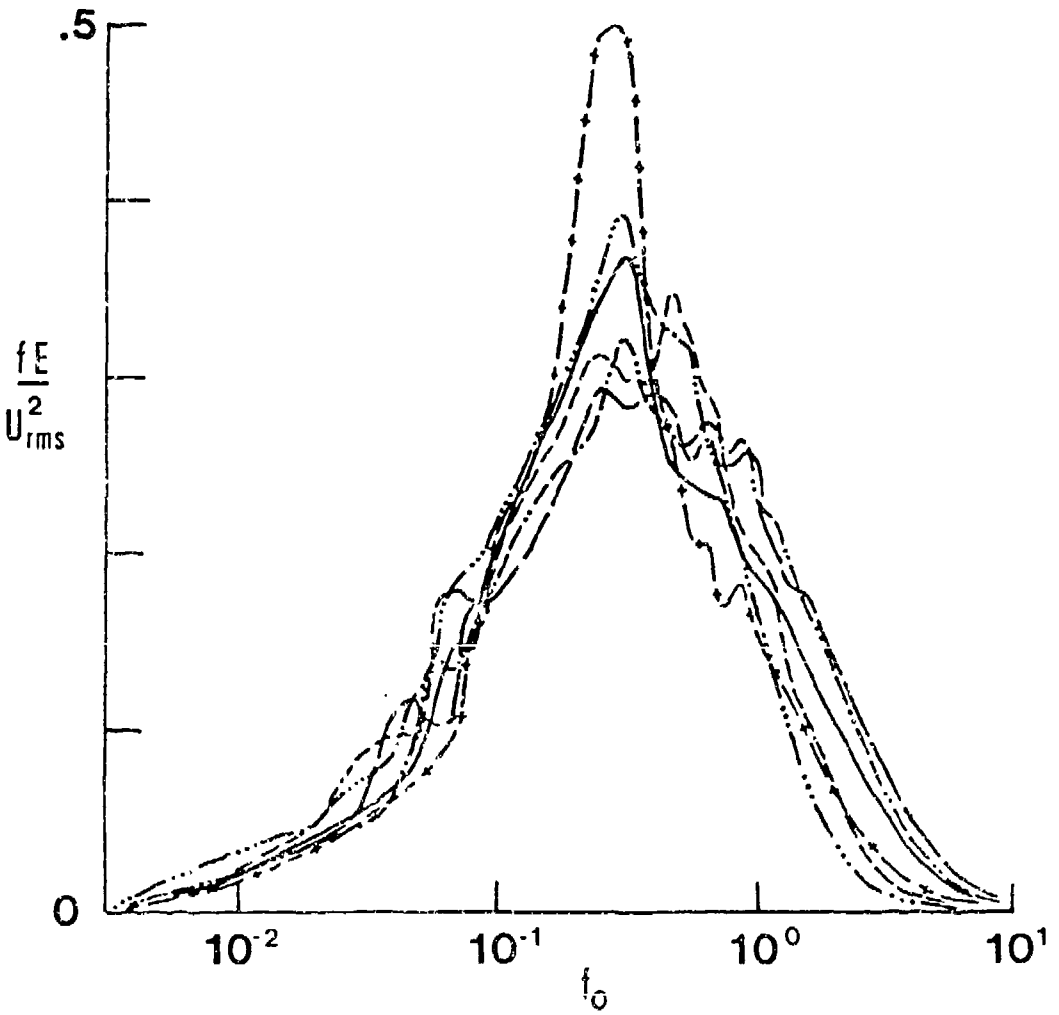

Figure 8. Streamwise Velocity Spectra at Different Distances from the Wall in a Cylindrical Boundary Layer: $R_\theta \approx 2000$: · ··· - ·· - ··· $y_+ \approx 2$; - - - - $y_+ \approx 13$; - ·· - ·· - ·· $y_+ \approx 37$; – – – – – $y_+ \approx 78$; ——— $y_+ \approx 158$; – + – + – + $y_+ \approx 399$

[Lueptow and Haritonidis.[31] Reprinted with the permission of the American Institute of Physics, copyright 1987.]

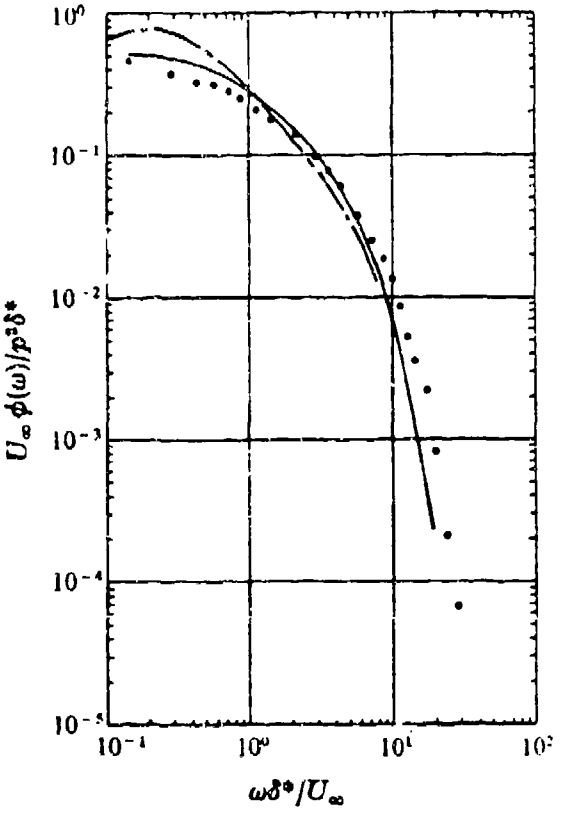

Figure 9. Wall Pressure Spectrum in a Cylindrical Boundary Layer [Willmarth and Yang.[14] Data points are measured for a cylindrical boundary layer $\delta/a \approx 2$. Solid and dashed lines are two different measurements for a planar boundary layer.[77,78] $\phi(\omega)$ is the power spectrum, ω is the angular frequency, and p is the turbulent wall pressure. Reprinted with the permission of the Cambridge University Press, copyright 1970.]

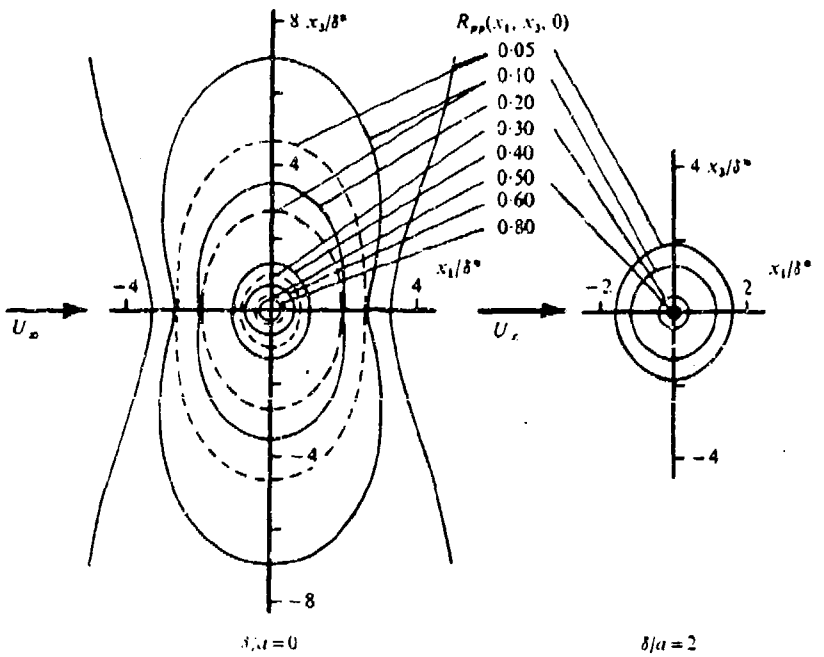

Figure 10. Effect of Transverse Curvature on Contours of Constant Wall Pressure Correlation [Willmarth and Yang.[14] Solid and dashed lines are two different measurements for a planar boundary layer.[77,79] $R_{pp}(x_1,x_3,0)$ is the normalized spatial wall pressure correlation at zero separation time; x_1 is the streamwise coordinate; x_3 is the spanwise coordinate. Reprinted with the permission of the Cambridge University Press, copyright 1970.]

4. STRUCTURE OF TURBULENCE IN A CYLINDRICAL BOUNDARY LAYER

Like a planar boundary layer, an understanding of the underlying structure of the turbulence in a cylindrical boundary layer is fundamental, yet difficult. Very little information is available on the structure of turbulence in a cylindrical boundary layer, although some aspects are becoming more clear.

4.1 EVENT DETECTION

Lueptow and Haritonidis[31] used VITA,[84] or variable interval time averaging, an event sampling technique based on the detection of layers of high shear, to detect burst cycles which are believed to be responsible for generating most of the turbulent velocity fluctuations in a planar boundary layer.[85] The ensemble averaged events detected using VITA for $\delta/a \approx 8$ resemble those constructed for a planar boundary layer and channel flow. This similarity suggests that the mechanism for the generation of turbulence at the wall is similar in all wall-bounded flows. The scaling for the frequency of bursts detected using VITA can be used to indicate whether the mechanism for the generation of turbulence scales with inner or outer variables. Although their data are inconclusive, Lueptow and Haritonidis found that outer scaling provides somewhat better collapse than inner scaling, suggesting that the outer flow affects events at the wall. By comparison, the burst frequency in a planar boundary layer scales with inner variables.

Lueptow and Haritonidis[31] also carried out uv-quadrant event detection based on sorting pairs of u and v into appropriate quadrants of the u-v plane to represent contributions to the Reynolds stress.[86] Quadrants 2 and 4 are associated with components of the burst cycle. Like VITA detected events, ensemble averages of uv-quadrant detected events are similar to those of other wall-bounded flows. In addition, the fractional contribution of each quadrant in the u-v plane to the Reynolds stress near the wall ($y_+ \approx 39$) is qualitatively similar to that for a planar boundary layer. Specifically, quadrant 2 events (negative u and positive v) represent the largest contribution to the Reynolds stress and correspond to the lift-up of low speed fluid during the burst cycle. Again the similarity of the results of event detection in a cylindrical boundary layer using the uv-quadrant technique with those of a planar boundary layer suggest that the mechanism for the generation of turbulence near the wall is similar.

4.2 SPACE-TIME VELOCITY CORRELATIONS

Measurements of the correlation of velocity at different azimuthal locations in a cylindrical boundary layer were made by Lueptow and Haritonidis.[31] In these experiments the streamwise velocity

was measured using three hot-wire probes located near the wall at three azimuthal locations that were 90° apart and at several streamwise spacings for flow conditions resulting in δ/a=8. The results of the experiments indicate that the correlation between any two probes is negative. This result is curious since the spanwise correlation in a planar boundary layer is positive. The authors suggest that the negative correlation may be a result of the splitting of a sweep of fluid around the cylinder pushing low-speed fluid ahead of it and resulting low-speed and high-speed flow 90° apart from each other. As would be expected, velocities at probes separated by 90° are better correlated than velocities at probes on opposite sides of the cylinder (separated by 180°). The velocities appear correlated over distances of at least 13 diameters suggesting that high- and low-speed lumps of fluid travel in adjacent parallel paths. The advection velocity determined from the cross-correlations was nearly the same as the local mean velocity.

Finally, VITA event detection on the velocity at the probes positioned near the wall (y_+=8) and probes positioned further from the wall (y_+=77) was used to determine the relationship between inner and outer events. Regardless of whether an upstream event occurs near the wall or a short distance from the wall, it seems to be a precursor to downstream events suggesting an interaction between the outer flow and the flow near the wall.

4.3 FLOW VISUALIZATION

Flow visualization of a cylindrical boundary layer has been accomplished by moving a flexible cylinder axially through a quiescent fluid. Lueptow and Haritonidis[31] used a system in which a very long O-ring moved around four pulleys located at the corners of a rectangular frame. One of the pulleys was driven by a dc motor. The frame was lowered into a tank of water so that the bottom two pulleys and the portion of the O-ring between them were submerged. A "hydrogen bubble" wire was positioned perpendicular to and just above the O-ring as it moved through the tank of water (δ/a≈24). In spite of the buoyancy of the bubbles, groups of bubbles were occasionally carried by the turbulence below the O-ring as shown in figure 11. The frequency of these events is of the same order of magnitude as the frequency of VITA events in which the fluid is decelerating in the streamwise direction. The authors point out that this type of turbulent transport is quite different from that of a planar boundary layer where the motion of large-scale structures is constrained by the wall. As δ/a becomes large, these coherent structures can travel from one side of the cylinder to the other with relative ease.

Other researchers have used birefringent liquids to observe the flow field surrounding moving filaments. Gebart and Hornfeldt[87] studied annular flow in a pipe with a nylon filament at the centerline of

the pipe acting as a moving inner boundary condition. The relationship of their results to a cylindrical boundary layer are difficult to ascertain because of the outer pipe wall boundary condition. Sakiadis[86] provides one photo of the flow field surrounding a moving thread, but it appears that the flow pictured is laminar.

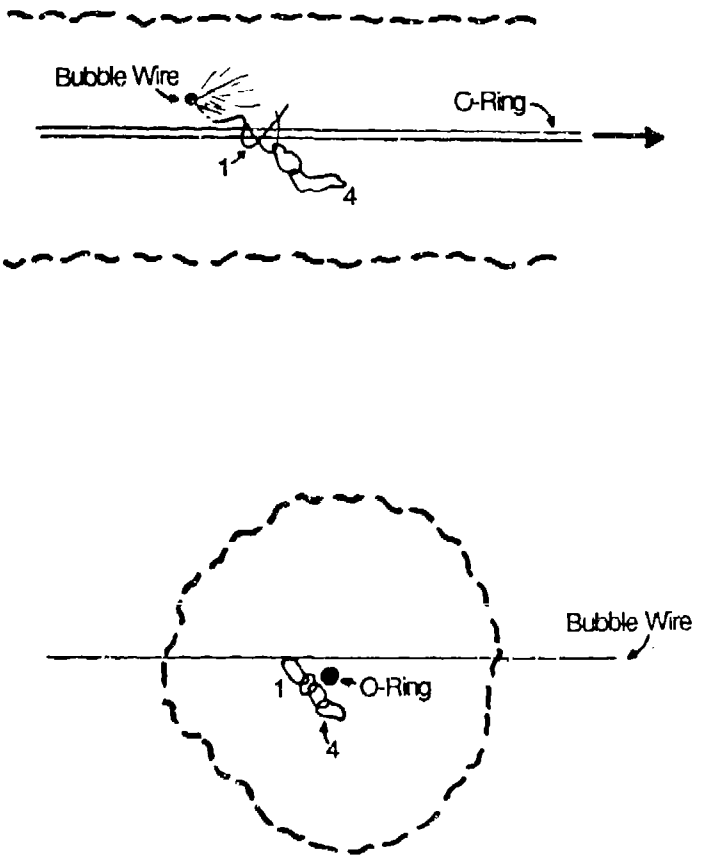

Figure 11. Sketches of the Motion of Large Structures in a Cylindrical Boundary Layer

[Upper: Side view of a cylinder (a long O-ring) moving to the right through quiescent water. A wire just above the cylinder and perpendicular to the plane of the paper generates bubbles. Lower: End view of a cylinder (O-ring) moving out of the plane of the paper. A wire just above the cylinder and in the plane of the paper generates bubbles. In both cases the sketches indicate a sequence of four positions of a small group of bubbles as the turbulent fluctuations carry them below the cylinder (positions 1 and 4 are labeled). Note that gravity is downward in the sketches, so the turbulent transport carries the bubbles in a direction opposite to their buoyancy. The dashed lines indicates the approximate edge of the boundary layer. Sketches are based on flow visualization by Lueptow[74] for $a_+ \approx 30$, $R_a \approx 600$, $\delta/a \approx 20$, time between positions=0.5 seconds.]

5. SUMMARY

A description of the boundary layer on a cylinder in axial flow has evolved over the past 30 years of research on the subject, but the present understanding of the flow lags behind that of other wall-bounded flows. This is a consequence of the difficulty brought about by the introduction of an additional length scale, the transverse curvature.

In the viscous sublayer, the transverse curvature results in an equation for the mean velocity that is different from the planar law, although it approaches the planar law as the radius of the cylinder increases (equation 2-3). Away from the wall the effect of transverse curvature becomes pronounced as the mean velocity profile becomes fuller. When plotted in planar wall coordinates this appears as a log law relationship with the slope of the logarithmic region decreasing as the transverse curvature decreases. Yet the parameter of interest, the transverse curvature, is precisely the most troublesome parameter of the flow. The appropriate scaling for the wall-normal coordinate has not been clearly defined.

Like scaling laws, appropriate nondimensional parameters remain elusive. Although several nondimensional parameters were suggested early in this paper, the evidence supporting one over the others is weak. The radius Reynolds number , R_a, has already been shown to be the least appropriate nondimensional parameter, since it omits any effect due to varying wall shear stresses or integral thicknesses at different axial positions. For this reason a_+ appears to be an attractive parameter, but Lueptow et al.[10] point out that a wide range of mean velocity profile data collapse better with δ/a than with a_+. Both δ/a and a_+ suffer from the difficulty that measurements of the boundary must be made to determine these parameters. This is similar to the problem of using the momentum thickness instead of the streamwise position for the length scale in the Reynolds number for a planar boundary layer -- the momentum thickness length scale requires making a measurement. The laminar cylindrical boundary layer parameter, ξ, overcomes this deficiency. Except for Denli and Landweber,[8] employment of this parameter has been minimal so its usefulness is uncertain.

More certain is the wake-like character of a boundary layer on a very small cylinder. Denli and Landweber[8] describe it best. "If the boundary-layer thickness relative to the transverse radius of curvature is large, the cylinder may be considered as a small vorticity- and turbulence-producing disturbance. Consequently, the flow might be considered similar to a wake flow with the modified inner boundary condition. The important difference is that the drag generating the wake is a function of the longitudinal coordinate..." Luxton et al.[9] describe a cylindrical boundary layer further as a "continuously

regenerated wake." The wake-like character of a cylindrical boundary layer is clear, but the existence of an outer wake law is subject to debate as discussed earlier.

Although the outer flow is wake-like, the wall acts to continuously convert mean flow energy into turbulent energy at the wall of the cylinder. In fact, a cylindrical boundary layer is very effective at this conversion of energy as evidenced by a higher coefficient of friction for a cylindrical boundary layer than for a planar boundary layer at the same Reynolds number. Detection of the burst cycle (VITA and uv-quadrant detection schemes) as well as measurements of the turbulence intensity indicate that the mechanism for the generation of turbulence is similar in cylindrical and planar boundary layers.[31] This mechanism is the burst cycle[85] where low-speed fluid intermittently lifts up from the wall resulting in an unstable shear layer that violently breaks up generating turbulent velocity fluctuations followed by a sweep of fluid toward the wall.

Willmarth et al.[12] recall a proposal for a mechanism for the cyclic occurence of bursts in a planar boundary layer that suggests that the pressure fields resulting from large eddies passing over the sublayer produce a massaging action in a localized region that intermittently results in a burst. Since the convection velocity in a cylindrical boundary layer is the same as for a planar boundary in spite of the "fullness" of the cylindrical profile, the time scale of the massaging action is similar in a cylindrical boundary layer. Lueptow and Haritonidis[31] support the existence of this massaging action as evidenced by flow visualization of large scale coherent structures and velocity correlations between probes near the wall and further out in the boundary layer. They suggest that the outer fluid "may wash over the cylinder precipitating events on the sides of the cylinder." Luxton et al.[9] note that these washes of outer fluid may sweep away the inner layer maintaining vorticity in the layer very efficiently. Since the mixing in a cylindrical boundary layer is controlled by the inertia of the large eddies rather than by viscous effects associated with the wall, the profile of the mean velocity, Reynolds stress, and intermittency are altered from those of a planar boundary layer.

6. FURTHER RESEARCH

As evident throughout this report, the character of cylindrical boundary layers is poorly understood in comparison to planar boundary layers. Several potentially productive areas of research are outlined below.

- MEASUREMENT OF MEAN VELOCITY PROFILES
  - Mean velocity data are needed over a wider range of conditions.

In spite of the large number of measurements of the mean velocity profile, a definitive scaling law is elusive. This is a result of inference of scaling laws from poor experimental data and a lack of adequate theoretical models. For the most part, though, more experimental data over a wide range of experimental conditions is necessary. For instance, the data of Willmarth et al.[12] appears to cover a very wide range of nondimensional parameters. But the variation in parameters was achieved by the variation of the cylinder diameter and, to some extent, the free stream velocity. The streamwise location of the measurement for a given cylinder was not an independent variable. Ideally, mean velocity profile measurements should be made while varying the cylinder diameter (a), the free stream velocity (U_∞), and the streamwise measurement location (x). As Willmarth et al.[12] point out, "...experiments should be designed to provide sufficient data concerning the effects of transverse curvature to allow a complete empirical formulation of the mean flow field. This was possible in the two-dimensional [planar] only after sufficient data and understanding had accumulated." Further analysis of the presently available data may also be helpful.

- WALL SHEAR STRESS
  - Direct measurement of the coefficient of friction

The skin friction in a cylindrical boundary layer continues to be an unresolved issue. Since Richmond's work[7] no attempts at the direct measurement of the coefficient of friction have been made. It seems likely that technological advances since then may permit such measurements.

  - Compilation of drag measurements

Many measurements have been made on the drag of cylinders and fibers. These results could be compiled in a useful format to provide insight for an empirical relation for the skin friction on a cylinder.

-- Fluctuating wall shear stress

No measurements of the fluctuating wall shear stress on a cylinder have been made. Measurements using hot film shear stress probes should be made on cylinders of different diameters under varying flow conditions to fill this void.

-- Drag reduction

Techniques for drag reduction, such as large eddy break-up devices, streamwise riblets, or microbubble injection, could be tested in a cylindrical boundary layer. The cylindrical geometry has the added advantage of eliminating edge effects that are present in a planar boundary layer experiment.

• MEASUREMENT OF TURBULENT QUANTITIES

-- Measurements of the Reynolds stress, turbulence intensity, and velocity spectra

Measurements of the turbulent quantities in the boundary layer are more scarce than measurements of the mean velocity profile. Aside from measurement difficulties, the streamwise and wall-normal turbulence intensities as well as the Reynolds stress have been measured over only a very limited range of parameters. Extending these measurements over a wider range of parameters should provide needed insight into the character of a cylindrical boundary layer

-- Wall pressure fluctuations for $\delta/a>4$

Wall pressure fluctuations have only been measured for relatively large cylinders. Using miniature hearing aid microphones the wall pressure could be measured for much smaller cylinders. Arrays of microphones could be used to map contours of constant wall pressure correlations and to measure the low wavenumber portion of the wall pressure spectrum.

• FLOW NOISE REDUCTION

-- Techniques for reduction of low frequency velocity fluctuations

Lohman[41] noted a reduction in the kinetic energy of the velocity fluctuations at low wavenumbers when the boundary layer was exposed to a local transverse motion ($\delta/a=0.2$). This suggests that further investigation of a method for the reduction of wall pressure fluctuations based on local transverse motion of the wall may be worthwhile.

• STRUCTURE OF TURBULENCE

– Flow visualization to character outer structures

Flow visualization of cylinders of different diameters moving through a tank of quiescent water may provide the details of the burst cycle and the effect of outer eddies on the generation of turbulence at the wall for cases where the boundary layer thickness is much greater than the cylinder radius.

– Space-time correlations of velocity to characterize coherent structures

Measurements of the space-time correlations of velocity and wall pressure for cylinders of different diameters may provide an understanding of coherent structures in the flow field. Further event detection measurements including the measurement of the correlation between wall pressure events and velocity events may be helpful in providing insight into the wall pressure spectrum and its relationship to the burst cycle.

• MODELING OF CYLINDRICAL BOUNDARY LAYERS

-- Enhanced models of the integral thicknesses and skin friction

Past predictive models of the coefficient of friction have been based on very crude models of the boundary layer profile. These models could be improved and enhanced based on recent experimental data. Extension of these techniques to rough surfaces may be useful.

– Direct computer simulation of a cylindrical boundary layer

Advances in computational fluid dynamics may permit the direct computational simulation of a turbulent boundary layer on a cylinder. The turbulent boundary layer on a flat plate has been successfully modeled at a Reynolds number based on momentum thickness of up to 1410.[89] Similar techniques could be used for a cylindrical boundary layer. Commercially available computational fluid dynamics codes run on a supercomputer may provide useful first-order approximations to the flow.

• NON-AXISYMMETRIC BODIES

-- Effect of oval cross-section on a turbulent boundary layer

While most of the work described above has emphasized the boundary layer that develops on a cylinder, transverse curvature that is not axisymmetric has not been studied. For instance, the radius of transverse curvature at the ends of the major axis of a long, oval cross-section body will be much less than that at the ends of the minor axis. This may allow the isolation of the effects of the outer flow on the generation of turbulence from the effects of transverse curvature, since large-scale structures cannot pass as easily from one side of the oval cross-section body to the other side.

REFERENCES

1. E. V. Telfer, E.V., "Frictional Resistance and Ship Resistance Similarity," Quart. Trans. Inst. Naval Arch., vol. 92, 1950, p. 1.

2. H. V. Eckert, 'Simplified Treatment of the Turbulent Boundary Layer Along a Cylinder in Compressible Flow," J. Aero. Sci. , vol. 19, 1952, p. 23.

3. R. O. Reid and B. W. Wilson, "Boundary Flow Along a Circular Cylinder, "J. Hydraulics Div., Proc. ASCE, vol. 89 (HY3), 1963, p. 21. (Also published as Technical Report No. 204-4, National Engineering Science Company, Pasadena, CA, 1962.)

4. B. C. Sakiadis, "Boundary-Layer Behavoir on Continuous Solid Surfaces: III. The Boundary Layer on a Continuous Cylindrical Surface, AIChE J. vol. 7, 1961, p. 467.

5. R. A. Seban and R. Bond, "Skin-Friction and Heat-Transfer Characteristics of a Laminar Boundary Layer on a Cylinder in Axial Incompressible Flow," J. Aero. Sci., vol. 18, 1951, p. 671.

6. A. D. Young, The Calculations of the Total and Skin Friction Drags of Bodies of Revolution at Zero Incidence, R & M 1874, British A.R.C., 1939.

7. R. L. Richmond, "Experimental Investigation of Thick Axially Symmetric Boundary Layers on Cylinders at Subsonic and Hypersonic Speeds," Hypersonic Res. Proj. Memo. no. 39, Cal. Inst. Tech., 1957.

8. N. Denli and L. Landweber, "Thick Axisymmetri : Turbulent Boundary Layer on a Circular Cylinder, J. Hydronautics, vol. 13, 1979, p. 92.

9. R. E. Luxton, M. K. Bull, and S. Rajagopalan, "The Thick Turbulent Boundary Layer on a Long Fine Cylinder in Axial Flow," Aeronaut J., vol. 88, 1984, p. 186.

10. R. M. Lueptow, P. Leehey, and T. Stellinger, "The Thick, Turbulent Boundary Layer on a Cylinder: Mean and Fluctuating Velocities," Phys. Fluids, vol. 28, 1985, p. 3495. (Also see P. Leehey and T. S. Stellinger, "A Wake Law for an Axially Symmetric Turbulent Boundary Layer on a Cylinder. (unpublished), Mass. Inst. of Tech., Dept. of Ocean Engineering, 1978.)

11. G. N. V. Rao and N. R. Keshavan, "Axisymmetric Turbulent Boundary Layers in Zero Pressure-Gradient Flows," J. Appl. Mech., vol. 39, 1972, p. 25.

12. W. W. Willmarth, R. E. Winkel, L. K. Sharma, and T. J. Bogar, "Axially Symmetric Turbulent Boundary Layers on Cylinders: Mean Velocity Profiles and Wall Pressure Fluctuations," J. Fluid Mech., vol. 76, 1976, p. 35. (See also W. W. Willmarth, R. E. Winkel, T. J. Bogar, and L. K. Sharma, "Axially Symmetric Turbulent Boundary Layers on Cylinders: Mean Velocity Profiles and Wall Pressure Fluctuations," Dept. Aerospace Eng., Univ. Mich., Rep. no. 021490-3-T, 1975).

13. F. H. Clauser, F.H., "The Turbulent Boundary Layer," Adv. Appl. Mech., vol. 4, 1956, p. 1.

14. W. W. Willmarth and C. W. Yang, "Wall Pressure Fluctuations Beneath Turbulent Boundary Layers on a Flat Plate and a Cylinder," J. Fluid Mech., vol. 41, 1970, p. 47.

15. M. B. Glauert and M. J. Lighthill, "The Axisymmetric Boundary Layer on a Long Thin Cylinder, Proc. Royal Soc. London, A , vol. 230, 1955, p. 188.

16. Coles, D.E., "The Law of the Wall in Turbulent Shear Flow," 50 Jahre Grenzschichtforschung, (Braunschweig: F. Vieweg und Sohn), 1955, p. 153.

17. G. Kempf, "Flachenwiderstand [Surface Resistance]," Werft Reederei Hafen, vol. 5, 1924, p. 52.

18. G. Hughes, "Friction and Form Resistance in Turbulent Flow and a Proposed Formulation for Use in Model and Ship Correlation," Trans. Inst. Naval Arch. , vol. 96, 1954, p. 314.

19. E. E. Zajac, "Dynamics and Kinematics of the Laying and Recovery of Submarine Cable," Bell System Tech. J., vol. 36, 1957, p. 1129.

20. R. M. Kennedy, H. P. Bakewell, and W. C. Zimmermann, Normal and Tangential Hydrodynamic Drag of Very Thin Cylinders in Near Axial Flow, Naval Underwater Systems Center, New London, CT, NUSC Technical Report 6811, 31 January 1983.

21. E. H. Andrews and D. C. Cansfield, Unpublished work cited in Fibre Structure, edited by J.W.S. Hearle and R.H. Peters (London: Butterworths), 1963, p. 487.

22. J. Gould and F. S. Smith, "Air-Drag on Synthetic-Fibre Textile Monofilaments and Yarns in Axial Flow at Speeds up to 100 Metres Per Second," J. Text. Inst. , vol. 71, 1980.

23. C. C. Ni and R. J. Hansen, "An Experimental Study of the Flow-Induced Motions of a Flexible Cylinder in Axial Flow," J. Fluids Eng., vol. 389, 1978.

24. A. Ziabicki, Fundamentals of Fibre Formation, (London: John Wiley & Sons), 1976, pp. 177-186.

25. Y. D. Kwon and D. C. Prevorsek, " Melt Spinning of Fibers: Effect of Air Drag," J. Eng. Ind.,vol. 10, 1979, p. 73. (Also published in J. Appl. Poly. Sci., vol. 23, p. 3105.)

26. L. R. Glicksman, "The Dynamics of a Heated Free Jet of Variable Viscosity Liquid at Low Reynolds Numbers, J. Bas. Eng., vol. 90, 1968, p. 343.

27. M. Matsui, "Air Drag on a Continuous Filament in Melt Spinning," Trans. Soc. Rheology, vol. 20, 1976, p. 465.

28. Y. Sano and K. Orii, "Drag Coefficients of Filaments in Air Flow During the Spinning," Sen-i Gakkaishi, vol. 4, 1968, p. 212 (in Japanese with English abstract).

29. A. Selwood, "The Axial Air-Drag of Monofilaments," J. Text. Inst.,vol. 53, 1962, p. T576.

30. Y. S. Yu, "Effect of Transverse Curvature on Turbulent-Boundary Layer Characteristics," J. Ship Res., vol 2, 1958, p. 33.

31. R. M. Lueptow and J. H. Haritonidis, "The Structure of the Turbulent Boundary Layer on a Cylinder in Axial Flow," Phys. Fluids, vol. 30,1987, p. 2993.

32. N. Afzal and K. P. Singh, "Measurements in an Axisymmetric Turbulent Boundary Layer Along a Circular Cylinder," Aero. Quart., vol. 27, 1976, p. 217.

33. W. W., Willmarth, L. K. Sharma, and S. Inglis, The Effect of Cross Flow and Isolated Roughness Elements on the Boundary Layer and Wall Pressure Fluctuations on Circular Cylinders, Dept. Aerospace Eng., Univ. Mich., Rep. no. 014439-01, 1977.

34. G. N. V. Rao, "The Law of the Wall in a Thick Axisymmetric Turbulent Boundary Layer," J. Appl. Mech., vol. 34,1967, p. 237.

35. M. C. Joseph, J. A. McCorquodale, and K. Sridhar, "Power Law for Turbulent Cylindrical Boundary Layers, Aero. J. , vol. 75, 1971, p. 46.

36. E. J. Adomaitis, E.J., "Experimental Study of Axisymmetric Turbulent Flow of an Incompressible Fluid Over a Cylinder," Fluid Mech. Sov. Res., vol. 11, 1982, p. 1. (Also published in a nearly identical form as: 'Experimental Study of Axisymmetric Turbulent Flow of an Incompressible Fluid Around a Cylinder," Fluid Mech. Sov. Res. , vol. 9, no. 115.)

37. Y. T. Chin, J. Hulsebos, and G. H. Hunnicut, "Effect of Lateral Curvature on the Characteristics and Skin Friction of a Turbulent Air Boundary Layer With and Without Helium Addition," Proc. 1967 Heat Transfer and Fluid Mech. Inst (Stanford: Stanford U. Press), 1967, p. 394.

38. M. Yasuhara, "Experiments on Axisymmetric Boundary Layers Along a Long Cylinder in Incompressible Flow," Trans. Japan Soc. Aero. Space Sci., vol. 2, 1959, p. 72.

39. L. R. Bissonnette, and G. L. Mellor, "Experiments on the Behaviour of an Axisymmetric Turbulent Boundary Layer with a Sudden Circumferential Strain," J. Fluid Mech., vol. 63, 1974, p. 369.

40. Y. Furuya, I. Nakamura, S. Yamashita, and T. Ishii, "Experiments on the Relatively Thick, Turbulent Boundary Layers on a Rotating Cylinder in Axial Flows," Bull. JSME, vol. 20, 1977, p. 191.

41. R. P. Lohmann, "The Response of a Developed Turbulent Boundary Layer to Local Transverse Surface Motion," J. Fluids Eng. , vol. 98, series I,1976, p. 354.

42. G. N. V. Rao, Comment on "Mean Velocity Profile of a Thick Turbulent Boundary Layer on a Cylinder," AIAA J, vol. 12, 1974, p. 574.

43. D. M. Chase, "Mean Velocity Profile of a Thick Turbulent Boundary Layer Along a Circular Cylinder, AIAA J., vol. 10, 1972, p. 849 (Full paper available from NTIS as N72-18295).

44. D. M. Chase, Reply by author to P. Bradshaw and V.C. Patel, AIAA J., vol. 11, 1973, p. 894.

45. P. Bradshaw and V. C. Patel, Comment on "Mean Velocity Profile of a Thick Turbulent Boundary Layer Along a Circular Cylinder," AIAA J, vol. 11, 1973, p. 893.

46. H. H. Fernholz and T. Podtschaske, Einige uberlegungen zur geschwindigkeitsverteilung und zur wandreibung in inkompressiblen rotationssymmetrischen turbulenten grenzshichten mit querkrummung: Recent Developments in Theoretical and Experimental Fluid Mechanics, Berlin: Springer-Verlag, 1979, p. 427.

47. E. M. Sparrow, E. R. G. Eckert, and W. J. Minkowycz, "Heat Transfer and Skin Friction for Turbulent

Boundary-Layer Flow Longitudinal to a Circular Cylinder," J. Appl. Mech., vol. 30, series E, 1963, p. 37.

48. A. S. Ginevskii and E. E. Solodkin, "The Effect of Lateral Surface Curvature on the Characteristics of Axially-Symmetric Turbulent Boundary Layers," J. Appl. Math. Mech. (translation of Soviet PMM), vol. 22, 1958, p. 1169.

49. T. Cebeci, "Laminar and Turbulent Incompressible Boundary Layers on Slender Bodies of Revolution in Axial Flow, J. Basic Eng., vol. 92, 1970, p. 545.

50. V. C. Patel, "A Unified View of the Law of the Wall Using Mixing-Length Theory," Aero. Quart., vol. 24, 1973, p. 55.

51. F. M. White, R. C. Lessmann, and G. H. Christoph, "Analysis of Turbulent Skin Friction in Thick Axisymmetric Boundary Layers," AIAA J, vol. 11, 1973, p. 821.

52. T. Cebeci, "Eddy-Viscosity Distribution in Thick Axisymmetric Turbulent Boundary Layers," J. Fluids Eng., vol. 95, 1973, p. 319.

53. P. S. Granville, "Mixing Lengths or Eddy Viscosities for Thick Axisymmetric Turbulent Boundary Layers Near a Wall," J. Ship Res., vol. 31, 1987, p. 207.

54. H. Eickhoff, "The Influence of Transverse-Curvature on the Velocity Law in Thick Axisymmetric Turbulent Boundary Layer," Deutsche Forschungs-und Versuchsanstalt fur Luft-und Raumfahrt (DFVLR) Note 82-05, 1982 (available from NTIS as N82-30519).

55. R. M. Lueptow and P. Leehey, "The Eddy Viscosity in a Turbulent Boundary Layer on a Cylinder," Phys. Fluids, vol. 29, 1986, p. 4232.

56. E. R. Van Driest, "On Turbulent Flow near a Wall," J. Aero. Sci., vol. 23, 1956, p. 1007.

57. L. Landweber and M. Poreh, "Frictional Resistance of Flat Plates in Dilute Polymer Solutions," J. Ship Res., vol. 17, 1973, p. 227.

58. N. Afzal and R. Narasimha, "Axisymmetric Turbulent Boundary Layer Along a Circular Cylinder at Constant Pressure," J. Fluid Mech., vol. 74, 1976, p. 113.

59. N. Afzal and R. Narasimha, "Asymptotic Analysis of Thick Axisymmetric Turbulent Boundary Layers," AIAA J, vol. 23, 1985, p. 963.

60. H. R. Kelly, "A Note on the Laminar Boundary Layer on a Circular Cylinder in Axial Incompressible Flow," J. Aero. Sci., vol. 21, 1954, p. 634.

61. C. B. Millikan, "The Boundary Layer and Skin Friction for a Figure of Revolution," Trans. ASME, APM-54-3, 1932, p. 29.

62. L. Landweber, Effect of Transverse Curvature on Frictional Resistance, David Taylor Model Basin, Washington, DC, Report 689, March 1949.

63. C. Lui and Y. Dai, "Axisymmetrical Turbulent Boundary Layer Along a Slender Cylinder," J. Hydronautics, vol. 7, 1973, p. 133.

64. J. A. D. Ackroyd, "On the Analysis of Turbulent Boundary Layers on Slender Cylinders," J. Fluids Eng., vol. 104, 1982, p. 185.

65. F. M. White, "An Analysis of Axisymmetric Turbulent Flow Past Along Cylinder," J. Basic Eng., vol. 94, 1972, p. 200. (Also published as The Axisymmetric Boundary Layer on an Extremely Long Cylinder, Naval Underwater Sound Laboratory, Report No. 1058, 1969).

66. A. M. Abdelhalim, U. Ghia, and K. N. Ghia, "Analysis of Turbulent Flow Past a Class of Semi-Infinite Bodies," J. Fluids Eng., vol. 108, 1986, p. 157.

67. J. R. Shanebrook and W. J. Sumner, "Entrainment Theory for Axisymmetric, Turbulent, Incompressible Boundary Layers," J. Hydronautics, vol. 4, 1970, p. 159.

68. P. S. Granville, Similarity-Law Entrainment Method for Thick Axisymmetric Turbulent Boundary Layers in Pressure Gradients, David Taylor Naval Ship Research and Development Center, Bethesda, MD, Report 4525, December 1975.

69. H. Schlichting, Boundary Layer Theory, McGraw-Hill Book Company, NY, 1979, pp. 692-695.

70. K. Karhan, "The Axial Frictional Resistance of Long Cylinders In turbulent Flow," J. Ship Res., vol. 4, 1959, p. 24.

71. D. B. Spalding, "A Single Formula for the 'Law of the Wall,"J. Appl. Mech., vol. 28, 1961, p. 455.

72. V. C. Patel, A. Nakayama, and R. Damian, "Measurements in the Thick Axisymmetric Turbulent Boundary Layer Near the Tail of a Body of Revolution," J. Fluid Mech., vol. 63, 1974, p. 345.

73. P. S. Klebanoff, Characteristics of Turbulence in a Boundary Layer With Zero Pressure Gradient, NACA Report 1247, 1955.

74. R. M. Lueptow, "The Turbulent Boundary on a Cylinder in Axial Flow," Sc.D Thesis, Mech. Eng. Dept., Mass. Inst. of Tech., 1986.

75. H. P. Bakewell, "Turbulent Wall-Pressure Fluctuations on a Body of Revolution," J. Acous. Soc. Amer., vol. 43, 1968, p.1358.

76. R. L. Parton, A. L. Goldman, R. L. Lowery, and M. M. Reischman, "Low-Frequency Pressure Fluctuations in a Axisymmetric Turbulent Boundary Layers," J. Fluid Mech., vol. 97, 1980, p. 299.

77. M. K. Bull, "Wall-Pressure Fluctuations Associated With Subsonic Turbulent Boundary Layer Flow," J. Fluid Mech., vol. 28, 1967, p. 719.

78. W. W. Willmarth and F. W. Roos, "Resolution and Structure of the Wall Pressure Field Beneath a Turbulent Boundary Layer," J. Fluid Mech., vol. 22, 1965, p. 81.

79. W. W. Willmarth and C. E. Wooldridge, "Measurements of the Fluctuating Pressure at the Wall Beneath a Thick Turbulent Boundary Layer," J. Fluid Mech., vol. 14, 1962, p.187.

80. W. K. Blake, Aero-Hydroacoustics for Ships, David Taylor Naval Ship Research and Development Center, Bethesda, MD, June 1984, pp. 698-703. Also published as Mechanics of Flow-Induced

Sound & Vibration. Academic Press, 1986.

81. D. M. Chase and C. F. Noiseux, "Turbulent Wall Pressure at Low Wavenumber: Relation to Nonlinear Sources in Planar and Cylindrical Flow," JASA, vol. 72, no. 3, 1982, p. 975.

82. M. R. Dhanak, "Turbulent Boundary Layer on a Circular Cylinder: the Low-Wavenumber Surface Pressure Spectrum Due to a Low-Mach-Number Flow," J. Fluid Mech., vol. 191, 1988, p. 443.

83. G. N. V. Rao, " Hydrodynamic Stability of a Laminar Boundary Layer With Transverse Curvature Effect," ZAMM, vol. 47, 1967, p. 427.

84. R. F. Blackwelder and R. E. Kaplan, "On the Wall Structure of the Turbulent Boundary Layer," J. Fluid Mech., vol. 76, 1976, p. 89.

85. S. J. Kline, W. C. Reynolds, F. A. Schraub, and P. W. Runstadler, "The Structure of Turbulent Boundary Layers," J. Fluid Mech. vol. 30, 1967, p. 741.

86. W. W. Willmarth and S. S. Lu, "Structure of the Reynolds Stress Near the Wall," J. Fluid Mech., vol. 55, 1972, p. 65.

87. R. Gebart and J. Hornfeldt, "Visualisation and Measurements on Laminar and Turbulent Annular Pipe Flow With a Moving Inner Boundary," Dept. Mechanics, Royal Inst. Tech., Stockholm, Report TRITA-MEK-84-06, 1984.

88. B. C. Sakiadis, "Boundary-Layer Behavoir on Continuous Solid Surfaces: I. Boundary-Layer Equations for Two-Dimensional and Axisymmetric Flow," AIChE J. vol. 7, 1961, p. 26.

89. P. R. Spalart, "Direct Simulation of a Turbulent Boundary Layer Up to R_θ=1410," J. Fluid Mech., vol. 87, 1988, p. 61.

BIBLIOGRAPHY OF RELATED REFERENCES

Crane, L.J., "Boundary Layer Flow on a Circular Cylinder Moving in a Fluid at Rest," J. Appl. Math. Phys. (ZAMP), vol. 23, 1972, p. 201.

Griffith, R. M., "Velocity, Temperature, and Concentration Distributions During Fiber Spinning," Ind. Eng. Chem. Fund., vol. 3, 1964, p. 245.

Jaffe, N.A. and T. T. Okamura, "The Transverse Curvature Effect on the Incompressible Laminar Boundary Layer for Longitudinal Flow Over a Cylinder," J. Appl. Math. Phys. (ZAMP), vol. 19, 1968, p. 564.

Koldenhof, E.A., "Laminar Boundary Layers on Continuous Flat and Cylindrical Surfaces," AIChE J, vol. 9, 1963, p. 411.

Neradka, V., "An Improved Method for the Calculation of Laminar, Axisymmetric, Incompressible Boundary Layer," ASME Paper 70-Flcs-13, 1970.

Probstein, R. F., and D. Elliott, "The Transverse Curvature Effect in Compressible Axially Symmetric Laminar Boundary-Layer Flow, J. Aero. Sci., vol. 23, 1956, p. 208.

Sears W. R., "The Boundary Layer of Yawed Cylinders," J. Aero. Sci., vol. 15, 1948, 49.

Seban, R. A., and R. Bond, "Skin-Friction and Heat-Transfer Characteristics of a Laminar Boundary Layer on a Cylinder in Axial Incompressible Flow," J. Aero. Sci., vol. 18, 1951, p. 671.

Stewartson, K., "The Axymptotic Boundary Layer on a Circular Cylinder in Axial Incompressible Flow," Quart. Appl. Math., vol. 13, 1955, p. 113.

Vasudevan, G., and Middleman, "Momentum, Heat, and Mass Transfer to a Continuous Cylindrical Surface in Axial Motion," AIChE J. vol. 16, 1970, p. 614.

INITIAL DISTRIBUTION LIST

Addressee	No. of Copies
DTIC	12
CNA	1
University of Connecticut, Dept. of Mechanical Engineering Storrs, CT (Prof. J. Bennett)	1
Johns Hopkins University Applied Physics Laboratory Laurel, MD 20707 (Mr. J. Lombardo, STA)	1
MIT, Dept. of Aeronautics and Astronautics Cambridge, MA 02139 (Prof. J. H. Haritonidis)	1
MIT, Dept. of Mechanical Engineering Cambridge, MA 02139 (Prof. P. Leehey)	1
University of Michigan Gas Dynamics Laboratory 218 Aeronautical Engineering Building Ann Arbor, MI 48109-2140 (Prof. W. Willmarth)	1
Northwestern University Dept. of Mechanical Engineering Evanston, IL 60208 (Prof. R. M. Lueptow)	5
NASA Langley Research Center Building 1247A Hampton, VA 23665 (Dr. D. Bushnell)	1
Office of Naval Research 800 N. Quincy Street, BCT #1 Arlington, VA 22217-5000 (Mr. J. Fein, Dr. R. J. Hansen, Code 1215)	2